Quart. J. R. Met. Soc. (1974), **100**, 76-108

551.510.53:551.513.1:551.515.11:551.524.733

Planetary-scale disturbances in the polar winter stratosphere

By A. J. SIMMONS*

Department of Applied Mathematics and Theoretical Physics, University of Cambridge

(Manuscript received 19 April 1973; in revised form 27 September 1973)

SUMMARY

Some models of steady planetary-scale disturbances forced in the winter stratosphere by tropospheric pressure perturbations are presented for zonal flows with both vertical and meridional shear. The resulting structure of these disturbances is realistic. In particular, they are confined in the horizontal to regions of strong westerly wind, and do not exhibit a deficient vertical penetration, results in contrast with some earlier studies. Examples are included in which amplitudes are insensitive to the presence of either a strong Newtonian cooling or singular-line absorption.

The time-dependent behaviour of stratospheric planetary waves is examined for a zonal wind with uniform vertical shear. Analytical solutions emphasize the importance of a low-level conversion of zonal available potential energy in amplifying a disturbance forced at the tropopause. When allowance is made for the meridional structure of the stratospheric jet, a reasonable agreement is obtained between theory and observation, in particular with respect to perturbation geopotential heights observed in sudden warmings.

1. INTRODUCTION

Observations of the polar stratosphere have revealed the presence in winter of marked planetary-scale disturbances superimposed on westerly winds which increase with height from the tropopause to the lower mesosphere. These disturbances comprise both relatively steady distortions of the circumpolar vortex, such as the Aleutian anticyclone, and transient perturbations, an extreme example of which occurs with the ' sudden warming ' phenomenon discovered by Scherhag (1952). The further theoretical study of planetary waves in the winter stratosphere presented in this paper is appropriate at a time when our observational picture is being enhanced by the global measurement of stratospheric temperatures from satellites (see e.g. Barnett *et al.* 1972).

Meridional sections of a typical January-mean circulation in the polar stratosphere, and of the dominant wavenumber one and wavenumber two perturbations to this circulation, are presented for the region below 10 mb on Fig. 1, which is reproduced from Hirota and Sato (1969). The westerly ' polar-night ' jet is strongest at the uppermost level, with a maximum located close to 65°N. The disturbances have amplitudes whose meridional and vertical variations are notably close to those of the mean flow, and their phases tilt westward with increasing height. For the upper stratosphere and lower mesosphere, the cross-section of zonal wind presented by Murgatroyd (1969) shows westerlies increasing to a maximum greater than 80 $m\,s^{-1}$ which is attained near 45°N and at a height between 60 and 70 km. Green (1972) presents observational evidence of an increase in amplitude of wavenumber one up to between 50 and 60 km, with a decrease at greater heights.

Apart from some relatively detailed numerical studies (Byron-Scott 1967, Manabe and Hunt 1968, Miyakoda, Strickler and Hembree 1970), until recently much of the effort in seeking a theoretical description of stratospheric planetary waves has been concerned with steady disturbances forced by low-wavenumber perturbations in the troposphere. Thus, for steady, small-amplitude, adiabatic disturbances to a uniform zonal flow, Charney and Drazin (1961) found wave energy to be propagated vertically only when the zonal flow was

* Present address: U.K. Universities' Atmospheric Modelling Group, Department of Geophysics, University of Reading.

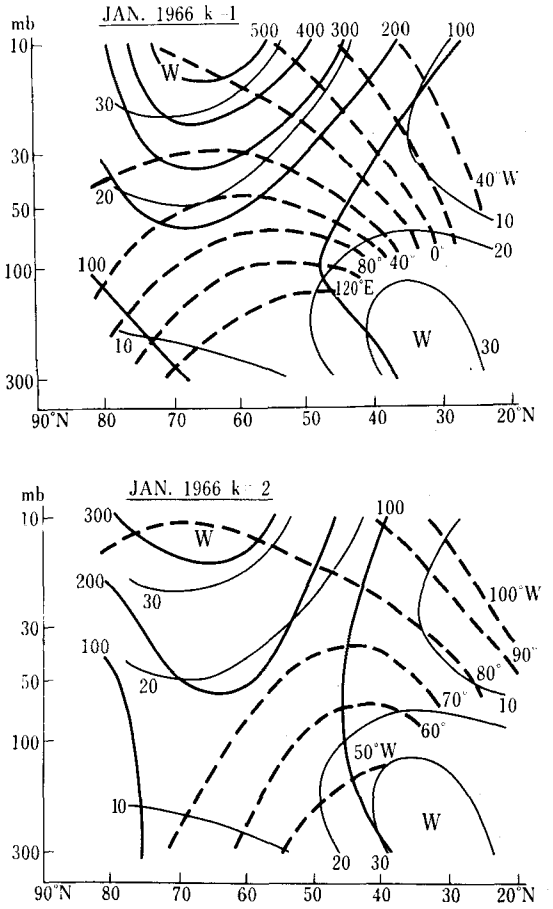

Figure 1. Meridional sections of monthly mean values of the zonal wind in $m\,s^{-1}$ (thin line), and the amplitude in metres (heavy full line) and phase angle of trough (broken line) of wavenumber one (top) and wavenumber two (bottom) for January 1966 (from Hirota and Sato 1969).

westerly relative to the phase speed of the perturbation, and less than a certain critical strength, which increased as the wavelength of the disturbance increased. These results are confirmed by the absence of significant disturbances in the summer stratospheric easterlies, and the predominance of only the lowest few wavenumbers in the polar-night westerlies. Charney and Drazin's conclusions were not qualitatively modified by their consideration of some examples in which the zonal flow varied with height.

Studies of steady planetary wave propagation in flows with meridional as well as vertical variations have been published by Dickinson (1968) and Matsuno (1970), with differing results. In a separable analytical model Dickinson found that vertically propagating waves were guided into regions where the zonal wind was westerly but relatively weak. In contrast, Matsuno found numerical solutions in which, at a given height, the maximum disturbance occurred close to the latitude of maximum zonal wind. The meridional structure obtained by Matsuno is in agreement with the observed monthly-mean state (see Fig. 1), but he found the vertical extent of his computed disturbances to be significantly less than is observed. This is most apparent in wavenumber two, but the observations discussed by Green (1972) show that the vertical penetration of wavenumber one was also underestimated.

A number of authors have investigated the response to a forcing whose amplitude varies with time. Hirota (1971) integrated numerically a linearized model of disturbances forced by a sinusoidally oscillating zonal flow, and found waves with a fluctuating amplitude much as observed. Dickinson (1970) considered the development in time of a critical level for horizontally propagating Rossby waves, and the vertical propagation of perturbations forced by an initial switch-on of a vertical velocity or temperature disturbance has been studied by Clark (1972) using some layered models. Matsuno (1971) has proposed a dynamical model of the stratospheric sudden warming in terms of forced wave motions and their interaction with the mean flow. He verified this with numerical integrations which simulated many features of the observed phenomenon.

In this paper we present some linearized models of planetary waves in idealized flows representative of the strong westerlies observed in the polar winter stratosphere. Following Dickinson and Matsuno, we do not consider details of the generation of low-wavenumber disturbances in the troposphere, but merely regard these disturbances as giving rise to pressure perturbations, supposed known, at the base of the stratospheric westerlies. Our analytical solutions for steady disturbances in flows with both meridional and vertical shear support Matsuno's finding that meridional variations in the curvature of the flow profile guide disturbances upward through the region of strongest westerlies. In addition, contrary to what might be inferred from Matsuno's study, our results show that a deficient vertical penetration is not an inevitable feature of the linearized theory of planetary wave propagation. Examples are presented in which the influence of Newtonian cooling and singular-line absorption on the vertical penetration is slight.

The time-dependent behaviour of planetary waves is analysed in a model with vertical shear in the zonal wind, but with no explicit representation of meridional shear. For adiabatic motions this model yields analytical solutions of relatively simple form, and it is easily adapted to include a height-independent Newtonian cooling. In general, our results give a qualitative picture of the response of the stratosphere to changes in low-wavenumber tropospheric disturbances. When a crude allowance is made for the meridional structure of the stratospheric westerlies, we obtain a reasonable quantitative agreement between theory and observation for the amplitudes of pressure perturbations associated with transient disturbances. In particular we find no indication of the deficiency in amplitude of wavenumber two found in Matsuno's (1971) simulation of a sudden warming.

2. Mathematical background

We consider, for the present, steady, small-amplitude, quasi-geostrophic perturbations to a stably-stratified zonal current $\bar{u}(y,z)$, taking x, y and z as eastward, northward and upward cartesian co-ordinates on a β-plane, although we later include results from a more realistic geometry. We assume a constant static stability, N^2, and a mean density $\rho(z)$ such that the scale height, $H_I, = -\rho(d\rho/dz)^{-1}$, is constant.

One of several derivations of the governing equations is that given by Charney and Drazin (1961). Considering a single wave component in the zonal direction, the horizontal velocity components u' and v' are given in terms of a perturbation stream function

$$Re\{\psi(y,z)e^{ikx}\},$$

a measure of the disturbance pressure p'. For adiabatic motions, the complex amplitude ψ satisfies the equation

$$\bar{u}\left\{\frac{1}{\rho}\left(\frac{\rho f^2}{N^2}\psi_z\right)_z + \psi_{yy} - k^2\psi\right\} + Q_y\psi = 0 \qquad . \qquad . \qquad (1)$$

expressing the conservation of quasi-geostrophic potential vorticity, where

$$Q_y = \beta - \bar{u}_{yy} - \frac{1}{\rho}\left(\frac{\rho f^2}{N^2}\bar{u}_z\right)_z , \qquad (2)$$

is the northward gradient of mean-flow potential vorticity. The vertical velocity, w', is given by

$$w' = -\frac{kf}{N^2} Re\{(\bar{u}\psi_z - \psi\bar{u}_z)ie^{ikx}\} ,$$

and the perturbation temperature, T', is proportional to ψ_z.

In the horizontal, the flow is bounded by vertical walls at $y = 0$ and $y = L$, giving

$$\psi(0,z) = \psi(L,z) = 0 .$$

At the lower boundary, $z = z_0$, we specify the amplitude of the stream function $\psi(y,z_0)$, a condition approximately equivalent to specifying the geopotential height pattern. The flow is unbounded above, and we require either that the energy density decrease,

$$\rho|\psi|^2 \to 0 \qquad \text{as } z \to \infty ,$$

or that wave energy is propagated away from source regions in the lower atmosphere:

$$\int_0^L \overline{p'w'}\,dy \geqslant 0 \qquad \text{as } z \to \infty ,$$

where the overbar denotes a zonal average.

Solutions to Eq. (1) are to be found without application of numerical methods to the full partial-differential equation, and this restricts our choice of the form of the mean flow, $\bar{u}(y,z)$. There is a straightforward separation of variables if $\bar{u}$ is a function of y or z alone (Charney and Drazin 1961), but more difficulty is encountered if both meridional and vertical variations are to be included. A separable model in such a case has been introduced by Dickinson (1968) who considered zonal winds of the form

$$\bar{u} \propto Q_y' \frac{U(y')V(z)}{V(z) + U(y')\tanh^2 y'}$$

where the latitudinal variable y' is given by

$$\tanh y' = \sin(\text{latitude}).$$

Since the northward gradient of mean-flow potential vorticity, Q_y', appears in this expression for $\bar{u}(y',z)$ in terms of the functions $U(y')$ and $V(z)$, in situations where the curvature terms in Q_y' are important, it is not easy to see how particular choices of $U(y')$ and $V(z)$ relate to the form of $\bar{u}(y',z)$. Thus as an alternative, in the β-plane geometry, we take $\bar{u}$ to be of the form

$$\bar{u}(y,z) = Y(y)Z(z) . \qquad (3)$$

Exact separable solutions are not in general possible for such a profile, but, if $Y(y)$ describes a jet-like variation of the mean flow in the horizontal and does not vanish in $0 < y < L$, the vertical and meridional structure of the disturbance may be separated in an approximation which may then be used iteratively to produce more accurate solutions. In practice it will be seen that convergence is rapid, and the first approximation surprisingly good. We shall assume a non-vanishing $Y(y)$ in the remainder of this Section, and in Sections 3 to 5. If $Y(y)$ vanishes in $0 < y < L$ the situation is modified by the possibility of an absorption

of wave energy due to the ' singular line ' where $Y(y) = 0$ (Dickinson 1968), and this case is discussed separately in Section 6.

The above-mentioned approximation is introduced by noting an exact separable solution when

$$\beta = 0\,, \qquad Y(0) = Y(L) = 0\,, \qquad \psi(y,z_0) = \Phi(z_0)Y(y)\,.$$

The solution of Eq. (1) is then

$$\psi(y,z) = \Phi(z)Y(y)$$

where Φ satisfies

$$Z\left\{\frac{1}{\rho}\left(\frac{\rho f^2}{N^2}\Phi_z\right)_z - k^2\Phi\right\} - \frac{1}{\rho}\left(\frac{\rho f^2}{N^2}Z'\right)_z \Phi = 0\,. \qquad . \qquad . \qquad (4)$$

Thus, in this much simplified case, the meridional structure of the disturbance is precisely that of the mean flow at all heights. In particular the disturbance attains its maximum at the latitude where the westerly wind is strongest. A similar tendency will be seen later to be a feature of several more general solutions. This finding is in agreement with both numerical studies (Matsuno 1970) and observations (Hirota and Sato 1969), and is in marked contrast to the suggestion of Dickinson (1968) that planetary waves will be guided along paths where the westerly wind is relatively weak. In the above example the meridional structure of the forced disturbances is determined by an exact cancellation of the $\bar{u}\psi_{yy}$ and the $-\psi\bar{u}_{yy}$ terms in Eq. (1), and an approximate cancellation occurs more generally. We attribute the differences between our results and those of Dickinson to his neglect of variations of Q_y' in assuming the zonal flow $\bar{u}$ to be modelled by the function $U(y')$ which appears in his latitudinal structure equation.

When $\beta \neq 0$, and $\psi(y,z_0)$ takes a more general form, a separation of variables is not possible. However, expanding

$$\left.\begin{aligned} \beta &= \beta_0 Y(y) + \sum_1^\infty \beta_n g_n(y) \\ \psi(y,z_0) &= \psi_0 Y(y) + \sum_1^\infty \psi_n g_n(y) \end{aligned}\right\}, \qquad . \qquad . \qquad . \qquad (5)$$

where the $g_n(y)$, together with $Y(y)$, form a complete orthogonal set, for realistic parameter values a good approximation is obtained by truncating the expansions (5) with only the $Y(y)$ terms present. There is then again a solution of the form

$$\psi(y,z) = Y(y)\Phi(z)\,,$$

where Φ now satisfies

$$Z\left\{\frac{1}{\rho}\left(\frac{\rho f^2}{N^2}\Phi_z\right)_z - k^2\Phi\right\} + \left\{\beta_0 - \frac{1}{\rho}\left(\frac{\rho f^2}{N^2}Z'\right)_z\right\}\Phi = 0\,, \qquad . \qquad . \qquad (6)$$

with $\Phi(z_0) = \psi_0$, and either $\rho\,|\Phi\,|^2 \to 0$ or $Im\{\Phi^*\Phi_z\} > 0$ as $z \to \infty$.

The examples presented in the following Section show Eq. (6) to yield a vertical structure close to that of the full solution for a flow with a sinusoidal meridional variation, and for two similar jet-like profiles. For a zonal flow $\bar{u} = Z(z)$ in a channel of width L, Charney and Drazin (1961) showed that, for a separable solution

$$\psi(y,z) = \Phi(z)\sin\frac{\pi y}{L}\,,$$

$\Phi(z)$ satisfies an equation of the form (6), but with the zonal wavenumber k replaced by the total wavenumber $\sqrt{k^2 + \pi^2/L^2}$, and β_0 by β. Thus, with a realistic latitudinal curvature

in the mean-flow profile, we find little qualitative modification to Charney and Drazin's conclusions. However, the reduction in wavenumber in the vertical structure equation, and consequent enhancement of the vertical penetration of disturbances forced from below, give rise to significant quantitative changes. A comparison of solutions for wavenumber two with and without meridional mean-flow curvature (Sections 3 and 7) shows the inclusion of curvature results in an increase of some 15 km in the height at which the disturbance attains its maximum amplitude.

A number of choices of $Z(z)$ which yield analytical solutions to Eq. (6) have been discussed by Charney and Drazin and we consider one of these in some detail, taking

$$Z(z) = \Lambda z\,,$$

Λ a constant vertical shear. This gives a reasonable approximation to the vertical structure of the polar-night westerlies over the lower and middle stratosphere, and the solutions in these regions are later shown not to depend critically on the unrealistically high westerly winds at large heights. Scaling z with f/Nk Eq.(6) becomes

$$z\{\Phi_{zz} - \mu\Phi_z - \Phi\} + \mu(1 + \beta_*)\Phi = 0\,, \quad . \quad . \quad . \quad (7)$$

where the dimensionless parameters are

$$\mu = \frac{f}{NkH_I}, \qquad \text{and} \qquad \beta_* = \frac{\beta_0 N^2 H_I}{f^2 \Lambda}.$$

The appropriate solution of Eq.(7) is

$$\Phi(z) = \Phi(z_0)\,\frac{z}{z_0}\,e^{-\lambda(z-z_0)}\,\frac{U(1-\gamma,2,2z\sqrt{1+\mu^2/4})}{U(1-\gamma,2,2z_0\sqrt{1+\mu^2/4})}, \quad . \quad . \quad (8)$$

where

$$\gamma = \frac{\mu(1+\beta_*)}{2\sqrt{1+\mu^2/4}}, \qquad \lambda = \sqrt{1+\mu^2/4} - \mu/2\,,$$

and $U(a,b,z)$ is the confluent hypergeometric function specified by Abramowitz and Stegun (1964).

We note that if parameter values are such that

$$U(1-\gamma,2,2z_0\sqrt{1+\mu^2/4}) = 0\,,$$

there is a resonant response to the forcing applied at $z = z_0$. This is a feature of more accurate solutions, and in such circumstances the steady, linearized, adiabatic theory is inappropriate. Further discussion of this resonance is given subsequently in the context of a time-dependent formulation.

In order to evaluate the accuracy of the approximate solution (8) comparison must be made with more accurate solutions, and this entails the inclusion of additional terms in the expansions (5) of β and $\psi(y,z_0)$. The resulting analysis is rather lengthy, and is outlined in an Appendix. We now discuss some specific solutions.

3. Wavenumber two

(a) *A sinusoidal jet*

We now consider flow on a β-plane centred at 60°N, with

$$\bar{u}(y,z) = \Lambda z \sin\frac{\pi y}{L}\,.$$

For a sinusoidal forcing,

$$\Psi(y,z_0) = \sin\frac{\pi y}{L},$$

and a channel width of 40° of latitude, Fig. 2 illustrates the dependence of the amplitude of wavenumber two on height at $y = L/2$ for three realistic values of the vertical shear. Other parameter values are $N^2 = 4{\cdot}5 \times 10^{-4}\,\mathrm{s}^{-2}$, and $H_I = 6{\cdot}5$ km, and the forcing level is $z_0 = 5$ km. In the absence of time-dependence, diabatic effects, or singular lines, there is no phase change with height, since the strong westerly winds at large heights trap disturbances of all wavelengths. For the shear of $2(\mathrm{m\,s^{-1}})\,\mathrm{km}^{-1}$, the approximate solution given by Eq.(8) is represented by a dashed line, and is seen to be close to the full solution. It is shown in the appendix that Eq. (8) gives the exact solution as the width of the channel, L, tends to zero, and we note a general insensitivity of the vertical penetration to the width of the sinusoidal jet.

In a model in which the vertical shear at the axis of the stratospheric jet varied between 1 and $1{\cdot}5\,(\mathrm{m\,s^{-1}})\mathrm{km}^{-1}$, Matsuno (1970) found a maximum in the geopotential height of a wavenumber two disturbance at about 25 km, in contrast with observations presented by Muench (1965) and Hirota and Sato (1969), both of which show disturbances increasing up to at least a height of 30 km. Since the zonally averaged wind is generally weak in the polar troposphere, we associate the level $z = 0$ in our model with the vicinity of the tropopause. This being so, some 5 to 10 km should be added to the vertical scale of Fig. 2 to obtain heights above ground level, and wavenumber two is then seen to attain a maximum at a height between 32 and 37 km when $\Lambda = 2\,(\mathrm{m\,s^{-1}})\mathrm{km}^{-1}$, and between 37 and 42 km when $\Lambda = 1{\cdot}5\,(\mathrm{m\,s^{-1}})\mathrm{km}^{-1}$. The vertical penetration of our solution is thus well in excess of that found by Matsuno, and in agreement with observation below 30 km. The occurrence of a maximum amplitude in the pressure disturbance (and a corresponding minimum amplitude, and phase change, in the temperature perturbation) between 30 and 40 km remains to be compared with detailed observational evidence when the latter becomes available for these greater heights.

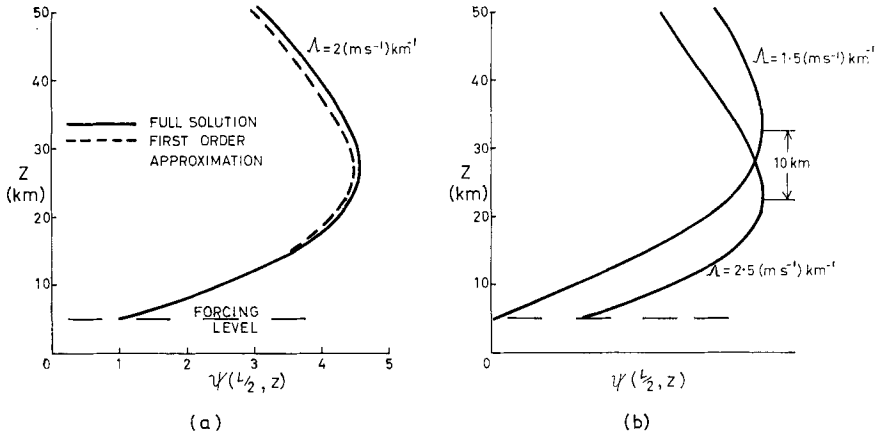

Figure 2. The variation with height of the amplitude at $y = L/2$ of steady wavenumber two disturbances to a zonal flow

$$\bar{u}(y, z) = \Lambda z \sin\frac{\pi y}{L}$$

at three values of the vertical shear. In (b) amplitudes are normalized owing to a resonance near $\Lambda = 1{\cdot}5$ $(\mathrm{m\,s^{-1}})\mathrm{km}^{-1}$. Parameter values are specified in the text.

(*b*) *Other meridional profiles*

Meridional sections of the zonal flows and amplitudes of wavenumber two disturbances are presented on Fig. 3 for the sinusoidal jet, and for the other profiles

$$\text{(i)} \quad Y_1(y) = \tfrac{5}{6} \sin \frac{\pi y}{L} - \tfrac{1}{6} \sin \frac{3\pi y}{L}, \qquad \text{and}$$

$$\text{(ii)} \quad Y_2(y) = 0{\cdot}796 \sin \frac{\pi y}{L} \left(1 - 0{\cdot}9 \cos \frac{\pi y}{L}\right).$$

In each case, $\psi(y,z_0) = \sin \pi y/L$, and $\Lambda = 2$ (m s^{-1}) km^{-1}. Profile Y_1 describes a sharper jet than is given by a sine function, whereas for profile Y_2, the southern wall is moved farther

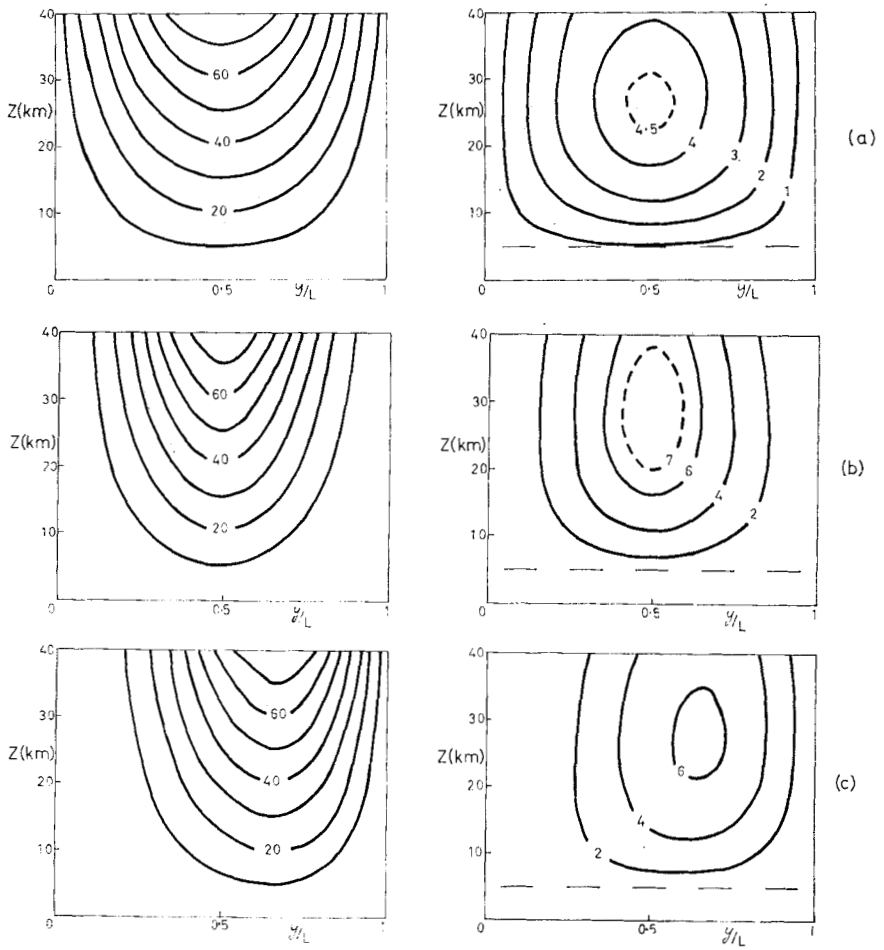

Figure 3. Meridional sections of zonal wind in m s^{-1} (left) and amplitude of wavenumber two (right) for flows with height-independent vertical shear, and meridional profiles

(a) $Y(y) = \sin \dfrac{\pi y}{L}$

(b) $Y(y) = Y_1(y) = \tfrac{5}{6} \sin \dfrac{\pi y}{L} - \tfrac{1}{6} \sin \dfrac{3\pi y}{L}$

and

(c) $Y(y) = Y_2(y) = 0{\cdot}796 \sin \dfrac{\pi y}{L} \left(1 - 0{\cdot}9 \cos \dfrac{\pi y}{L}\right)$.

from the axis of the jet, and the model represents the weaker westerlies which occur equatorwards of the polar-night jet in the middle stratosphere, although the particular form of the vertical structure of the mean flow employed for analytical convenience is unrealistic in this region.

Although the meridional variation of the forcing at z_0 differs from that of the mean flow for both profile Y_1 and Y_2, the meridional structure of the resulting disturbance is close to that of the mean flow at all but the lowest levels. As indicated by the analysis of Section 2, the disturbance is a maximum at the latitude where the westerly winds are strongest, with small amplitudes where the winds are weak. Interpreted in terms of the theory of planetary wave propagation, the negative meridional curvature of the flow profile near the axis of the jet enhances the β-effect and favours the vertical penetration of a disturbance originating at low levels; whereas the positive curvature, near the walls in profile Y_1, and to the south of the jet in profile Y_2, acts as a barrier to the spread of wave energy, as discussed by Matsuno (1970).

The vertical penetration of forced disturbances on a β-plane is insensitive to the meridional structure of the zonal flow for jet-like profiles similar to those shown on Fig. 3. Some indication of this is seen from the approximate solution (8), which has only a weak dependence on $Y(y)$ through the value of

$$\beta_0, = \beta \int_0^L Y(y)\, dy \Big/ \int_0^L Y^2(y)\, dy\,,$$

for $Y(0) = Y(L) = 0$. The analysis presented in the appendix shows the approximation to be particularly good when $z \gg f/Nk$, ≈ 9 km for wavenumber two, and examination of Fig. 3 reveals a remarkable similarity in the vertical structure of the disturbances, with a maximum attained within less than one kilometre of $z = 27$ km in all three cases.

(c) *A polar-cap geometry*

The assumptions required to obtain the β-plane approximation are not strictly satisfied by low-wavenumber perturbations in the polar stratosphere, but our conclusions are not significantly modified by results from a ' polar-cap ' geometry in which the region around the North Pole is mapped into cylindrical polar co-ordinates r, ϕ, and z, where $r = a\theta$, a = radius of the Earth, θ the co-latitude, and ϕ the longitude.

For zonal flows of the form

$$\bar{u}(r,z) = \Lambda z R(r), \qquad \text{Max } \{R(r)\} = 1\,,$$

several solutions for wavenumber two and $\Lambda = 2(\text{m s}^{-1})\text{km}^{-1}$ have been found by transforming the problem into that for the sinusoidal jet on a β-plane, as described in the Appendix. One such example is illustrated on Fig. 4. In comparison with earlier examples, we find minor differences in both the meridional and vertical structure of the forced disturbances. A general result, which may be seen on Fig. 4, is that the latitude at which the disturbance is a maximum is now found some 5° farther from the pole than the latitude of maximum zonal wind. This is a feature of monthly-mean observed disturbances (see Fig. 1), and may be interpreted as a consequence of the geometrical barrier to planetary wave propagation at the pole, where the local zonal wavelengths of all wavenumbers become small.

The wavenumber two disturbance illustrated on Fig. 4 attains its maximum at $z = 29$ km. Other examples attained maxima between 24 and 32 km, and we note a greater variation in the vertical penetration in the polar-cap geometry. There is now no exact cancellation as $z \to \infty$ of terms equivalent to $\bar{u}\psi_{yy}$ and $-\psi\bar{u}_{yy}$ in the β-plane geometry, but there is an approximate cancellation, and a general similarity in the vertical structure is found in the

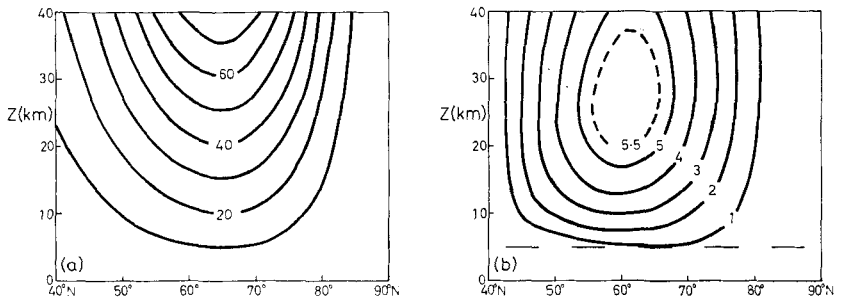

Figure 4. Meridional sections of zonal wind in m s^{-1} (left) and amplitude of wavenumber two (right) for flow in a polar cap-geometry, with

$$\bar{u}(r, z) = \Lambda z(r/R_0)^2 \, e^{1-4(r/R_0)^2}, \qquad 0 < r < R_0, \qquad R_0 \equiv 50° \text{ lat}.$$

two geometries. Such variations as do occur are no more than might arise from a different, but still realistic, choice of vertical wind shear within the range 1·5 to 2·5(m s^{-1})km^{-1}.

4. Wavenumber one

For the sinusoidal forcing, the amplitude at $y = L/2$ of the wavenumber one disturbance to the zonal flow

$$\bar{u}(y,z) = \Lambda z \sin \frac{\pi y}{L}$$

is shown on Fig. 5(a) for $\Lambda = 2$(m s^{-1})km^{-1}. The solution given by Eq.(8) is again seen to be very close to that obtained from higher order approximations, and both describe a disturbance whose amplitude increases well beyond the $z = 50$ km level, reaching a maximum close to 115 km, a height very much in excess of that found for wavenumber two.

In the winter hemisphere westerly winds increase up to a height of 60 to 70 km and thereafter decrease. It is thus appropriate at this stage to consider how our findings are modified when the model zonal flow, instead of increasing indefinitely with height, decreases above a certain level. From Eq.(6), solutions in terms of confluent hypergeometric functions have been obtained for a wavenumber one disturbance to a zonal flow

$$\left.\begin{aligned} \bar{u} &= \Lambda z \sin \frac{\pi y}{L} && , \quad 0 < z < H, \\ &= \Lambda(2H - z) \sin \frac{\pi y}{L} && , \quad H < z < H_1, \\ &= \Lambda(2H - H_1) \sin \frac{\pi y}{L} && , \quad H_1 < z \end{aligned}\right\} \qquad . \quad . \quad (9)$$

which attains a maximum at $z = H$, and then decreases to maintain a constant value above $z = H_1$. With $\Lambda = 2$(m s^{-1})km^{-1}, the vertical structure of disturbances when $H = 50$ km, $H_1 = 80$ km, and $H = 40$ km, $H_1 = 60$ km, are presented on Fig. 5(b). The model now permits an upward propagation of energy owing to the weak westerlies in $z > H_1$, but the strong westerlies near $z = H$ allow only a weak vertical flux, and, apart from a shift through 180° near $z = 10$ km, phase changes below 50 km are insignificant. With $H = 50$ km there is very little difference below 50 km between the solution illustrated for $H_1 = 80$ km and one with $H_1 = 90$ km. Above 50 km, the disturbances have an initial decrease in amplitude,

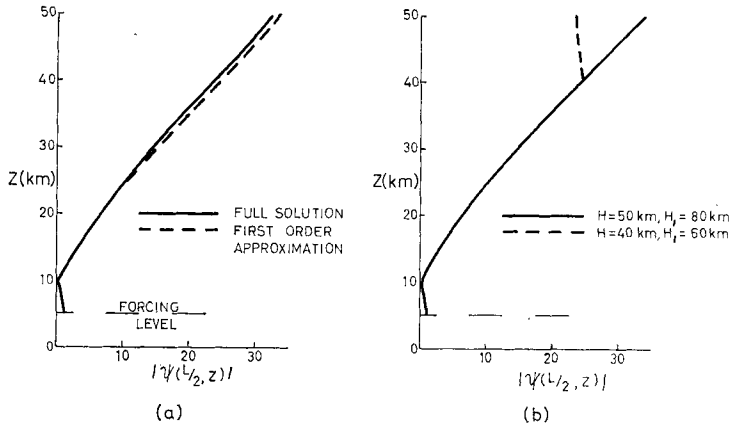

Figure 5. The variation with height of the amplitude at $y = L/2$ of steady wavenumber one disturbances to the zonal flows

(a) $\bar{u} = \Lambda z \sin \frac{\pi y}{L}$, $z > 0$, and

(b) $\bar{u} = \Lambda z \sin \frac{\pi y}{L}$, $H > z > 0$,

$= \Lambda(2H - z) \sin \frac{\pi y}{L}$, $H_1 > z > H$,

$= \Lambda(2H - H_1) \sin \frac{\pi y}{L}$, $z > H_1$, $\Lambda = 2(\text{m s}^{-1})\text{km}^{-1}$.

followed by an exponential increase at higher levels. Below 40 km the difference between the two solutions shown on Fig. 5(b) is less than 0·5 per cent of the maximum amplitude attained.

The results for profile (9) confirm the prediction of the constant shear model that the wavenumber one disturbance will increase with height throughout the region of eastward shear in the polar winter stratosphere, a result which again differs from that of Matsuno (1970). Above the 10 mb level, detailed observations of the dependence of the amplitude of wavenumber one on height are lacking, but data discussed by Green (1972) suggest that wavenumber one does indeed increase to a height of some 50 to 60 km, and thereafter decreases. Consistent with this result, and with geostrophic and hydrostatic balance, Labitzke (1972) notes that temperature changes in the winter stratosphere are accompanied by changes of opposite sign in the mesosphere. Some theoretical evidence for the high-level decrease in amplitude of the wavenumber one geopotential is seen on Fig.5(b), although the unrealistic height-independent winds above $z = H_1$, and neglect of dissipation, prevent any detailed comparison between theory and observation.

For very long wavelengths, a maximum disturbance amplitude close to the position of the zonal wind maximum is to be expected since, in regions where the curvature terms dominate the $\beta\psi$ and $\bar{u}k^2\psi$ terms in Eq.(1), we find the solution

$$\psi(y,z) \propto \bar{u}(y,z) . \quad . \quad . \quad . \quad . \quad (10)$$

Both the vertical and meridional variations of the disturbance geopotential are then similar to those of the mean flow.

Solutions with the zonal flow given by Eq.(9) have also been found for wavenumber two, and are generally similar at stratospheric levels to those discussed in Section 3. Addi-

tional examples with other choices of zonal wind at high levels, and a realistic drop in static stability at the model stratopause, confirm the insensitivity of solutions of the type presented here to the precise nature of the mean state at large heights (Simmons 1972).

5. Newtonian cooling

Owing to radiative and photochemical effects, temperature perturbations in the stratosphere tend to relax towards a state of thermal equilibrium. Lindzen and Goody (1965) estimated this to occur on a time-scale varying from about a fortnight near the tropopause to a week in the upper stratosphere; recent work by Blake and Lindzen (1973) suggests a more rapid relaxation above 30 km.

Dickinson (1969) has studied the vertical propagation of planetary waves with radiative damping approximated by a Newtonian cooling in which a diabatic heating $-\chi c_p T'$ is added to the perturbation thermodynamic equation. For a wide range of parameter values Dickinson found solutions for a uniform zonal flow. These indicated a strong attenuation of planetary waves during equinoctial periods when zonal winds are weak, and an attenuation of quantitative significance throughout the winter.

For a zonal flow with constant vertical shear, Newtonian cooling may be included in a straightforward manner if the parameter χ is independent of height (Simmons 1972), in which case solutions may again be found in terms of confluent hypergeometric functions. We adopt this simplification here, and present results for $\chi = 7\ (\text{day})^{-1}$ and $\chi = 14\ (\text{day})^{-1}$.

Solutions for a sinusoidal variation of the mean flow have been found in the approximation described in Section 2, where we expand χ in the same manner as β, (Eq.(5)), and again truncate with only the lowest meridional mode present. The vertical structure of the solution is again given by Eq.(8), but with γ redefined by

$$\gamma = \frac{\mu(1+\beta_*) - i\chi'}{2\sqrt{1+\mu^2/4}}, \qquad \chi' = \frac{4N\chi}{\pi f \Lambda},$$

and z replaced by $z - i\chi'$. For a vertical shear of $2(\text{m s}^{-1})\text{km}^{-1}$, the amplitude, phase, and dimensionless northward heat transport, of wavenumber one and wavenumber two are presented on Fig. 6. The inclusion of Newtonian cooling is seen to make little difference to the vertical penetration of the forced disturbances, which are somewhat reduced in amplitude.

Observations of the low-wavenumber disturbances in the polar winter stratosphere show a marked westward tilt of the lines of constant phase with increasing height (Muench 1965), and associated with this is a northward heat flux. Sawyer (1965) has discussed the necessity in winter of a poleward heat transport by large-scale eddies which balances the radiative cooling of polar regions, and he estimated that a covariance $\overline{v'T'}$ of 13 m °C s^{-1} is required at 50°N in the lower stratosphere. Values deduced by Newell *et al.* (1969) from observations show a transport in the polar-night jet of 10 m °C s^{-1} at 100 mb rising to 30 m °C s^{-1} at 10 mb. A spectral analysis of the heat transport at 25 mb shows most to be carried by wavenumber one (Anderson 1964).

The northward eddy heat transport by the steady, trapped, non-dissipative disturbances described in preceding sections is identically zero, and the heat fluxes associated with the propagating wavenumber one disturbances to profiles of the form of Eq. (9) are negligible. This is not true of the steady disturbances in the presence of Newtonian cooling. Allowing for a factor (wavenumber)^2 which must be inserted to dimensionalize the heat flux curves shown on Fig. 6, the theoretical description of an increase of the wavenumber one transport with height, and its dominance over that by wavenumber two, is in accord with observation.

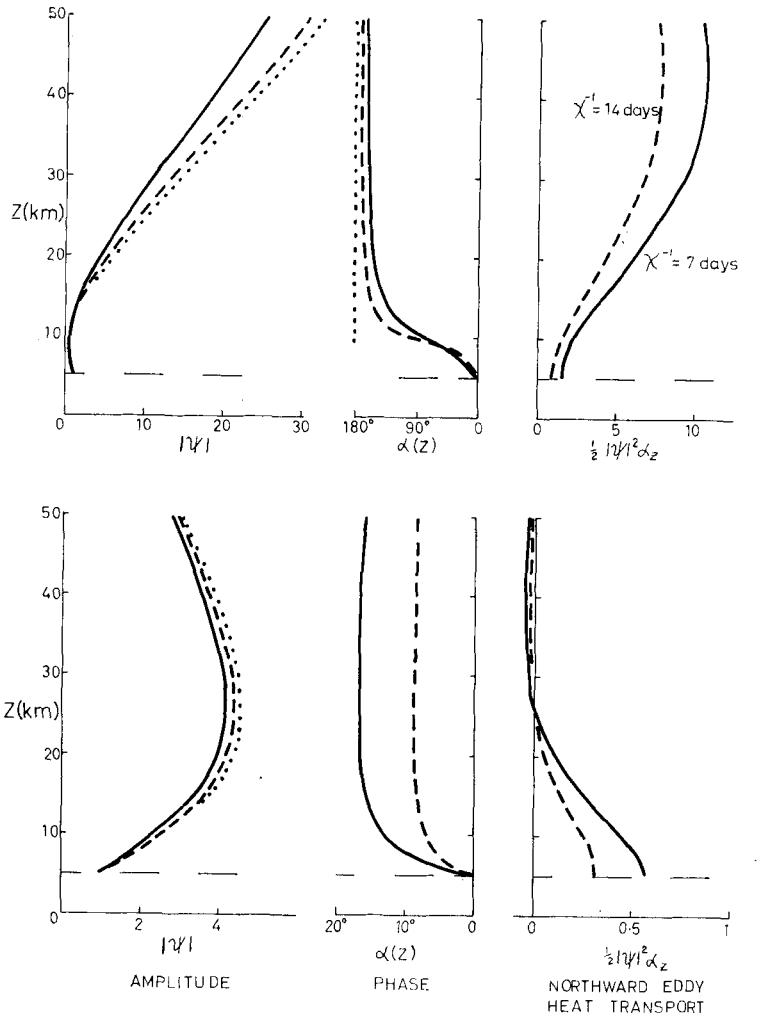

Figure 6. Solutions with Newtonian cooling. The variation with height at $y = L/2$ of the amplitude, $|\psi|$, (left), phase, $\alpha(z)$, (centre), and dimensionless northward eddy heat transport, $\frac{1}{2}|\psi|^2\alpha_z$, (right), for wavenumber one (upper) and wavenumber two (lower).

Dotted curves: adiabatic solutions.
Dashed curves: cooling time = 14 days.
Solid curves: cooling time = 7 days.

To evaluate the magnitude of the transport, forcing amplitudes of 100 m are assumed for the geopotential heights of both wavenumber one and wavenumber two at the $z = 5$ km level (which, as before, we identify somewhat loosely with the 100 mb pressure level). These values give disturbance amplitudes below 10 mb which are similar to observed values for the semi-permanent disturbances present in the time-height sections of wave amplitude presented by Muench (1965) and Hirota and Sato (1969). For $\chi = 7$ (day)$^{-1}$, a net transport of the order of 5m °C s^{-1} is found near the forcing level, rising to about 15m °C s^{-1} at $z = 20$ km (the ' 10 mb ' level), with values reduced by a factor of about two-thirds for a cooling time of 14 days. The semi-permanent disturbances in the presence of radiative cooling thus appear to account for about half the observed poleward heat transport in the polar

winter stratosphere. Significant heat transports are also associated with transient disturbances of the type to be discussed in Sections 7 and 8.

The steady, forced disturbances transport heat northwards in a region of westerly shear in the zonal flow. They are thus maintained in the presence of radiative dissipation not only by the work done by the forcing at the lower boundary, but also by the conversion of zonal to eddy available potential energy. For the solutions presented on Fig. 6, the latter accounts for 70 per cent of the net energy required per unit time to maintain wavenumber one when $\chi^{-1} = 14$ days, and 68 per cent when $\chi^{-1} = 7$ days. For wavenumber two, a figure of 84 per cent is found, for both cooling times. Thus, although the forcing plays an essential rôle in maintaining the disturbances, the bulk of the energy required for their continued existence is drawn from the mean state. The maximum extraction of energy takes place close to the forcing level, where the density, $\rho(z)$, is largest.

In addition to those illustrated, solutions have been found with cooling times as low as 3 days above $z = 20$ km, these being consistent with current estimates by Blake and Lindzen (1973) of cooling times in the upper stratosphere. Disturbance amplitudes are found to be reduced little compared with those illustrated for $\chi^{-1} = 7$ days. A much enhanced northward heat transport is found above $z = 20$ km, and the increased dissipation in the upper stratosphere is thus balanced by an increased conversion of available potential energy, with little reduction in the level of disturbance energy.

6. Singular-line absorption

Eq. (1) is singular along lines within the flow field where $\bar{u}(y,z) = 0$. In preceding Sections we have included zeros in the mean flow only when they coincide with the boundaries, in which case they are of no particular significance. However, Dickinson (1968) has shown that when singular lines occur away from walls, they cause wave energy to be absorbed, and he, and Matsuno (1970), have discussed how the equatorial zero-wind line might act to attenuate planetary-scale disturbances forced in the polar winter stratosphere. In this Section, we examine how our earlier results are modified by singular-line absorption.

We again consider zonal flows of the form (3), now allowing the possibility that $Y(y) = 0$ within the flow field. We discuss mostly the case of zero vertical shear, $Z(z) = U_0$, a constant, but mention also asymptotic solutions valid for large z for a flow with uniform vertical shear, $Z(z) = \Lambda z$. The horizontal structure, $Y(y)$, is restricted to forms for which analytical solutions may be found in the vicinity of the singular line, where difficulties are likely to be encountered with a numerical scheme. Although we are now envisaging flows of broad latitudinal extent, we retain the convenient β-plane approximation, since the highly idealized nature of the model zonal flow does not warrant geometrical sophistication.

When $Z(z) = U_0$, separable solutions to Eq. (1) take the form

$$\psi(y,z) = \Phi(y)e^{-\lambda z}, \qquad (11)$$

where, scaling y with L, and z with f/Nk,

$$Y\{\Phi_{yy} - \kappa^2\Phi\} + \{\beta_0 - Y''\}\Phi = 0, \qquad (12)$$

with

$$\lambda = -\mu/2 + \sqrt{1 + \mu^2/4 - \varepsilon\kappa^2}, \qquad (13)$$

$$\mu = \frac{f}{NkH_I}, \quad \varepsilon = \frac{1}{k^2L^2}, \quad \text{and} \quad \beta_0 = \frac{\beta L^2}{U_0}.$$

With walls at $y = y_l$ and $y = y_m$, the boundary conditions

$$\Phi(y_l) = \Phi(y_m) = 0 ,$$

together with Eq. (12), define an eigenvalue problem for the separation parameter κ^2. This eigenvalue, and the eigenfunction $\Phi(y)$ which determines the meridional structure of the disturbance, are independent of the zonal wavenumber k, which influences only the vertical structure.

On the basis of a separable model Dickinson (1968) asserted that there are no normal mode solutions for planetary wave propagation in the presence of singular lines. This is true, however, only when the separation parameter, κ^2 in our case, is assumed to be real. Dickinson's proof does not hold if the parameter is complex, and an examination of Eqs. (11) and (13) shows that a complex κ is, in fact, necessary in order that there be a convergence of the vertical energy flux,

$$\frac{\partial}{\partial z}(\overline{p'w'}) < 0$$

to balance the absorption of energy due to the singular line.

In regions where $Y(y)$ is a linear function of y, solutions to Eq. (12) may be obtained in terms of confluent hypergeometric functions, and these have been utilized to find solutions for several velocity profiles. One such profile is illustrated on Fig. 7, together with the resulting dependence of κ, which determines the vertical structure through Eqs. (11) and (13), on the dimensionless β-parameter, β_0, for the eigenvalue which describes the principal response to a general forcing, all other eigenvalues being associated with a more rapid exponential decay in the vertical. The curves for $y_l = -1$ and $y_l = 0$ illustrate cases with and without singular-line absorption. In the former example complex eigenvalues are indeed found, but with imaginary parts very much smaller than the real parts, and the similarity of the two $Re(\kappa)$ curves illustrates how little the vertical structure of the disturbance is modified when the vertical wall at $y_l = 0$ is removed to give a singular line and easterly flow to the south of the westerly jet.

Meridional cross-sections of wave amplitude are presented on Fig. 8 for wavenumber two with $U_0 = 40$ m s^{-1}, $L = 30°$ latitude, and other parameter values as used previously. The velocity profile is that shown on Fig. 7. The solutions have been expanded in series of eigensolutions of Eq. (12) truncated with five modes present, with amplitudes chosen to give least-squares fits to the forcing function

$$\psi(y,z_0) = Y(y) \quad , \quad 0 < y < 2 \; ; \; \psi(y,z_0) = 0 \quad , \quad y < 0 .$$

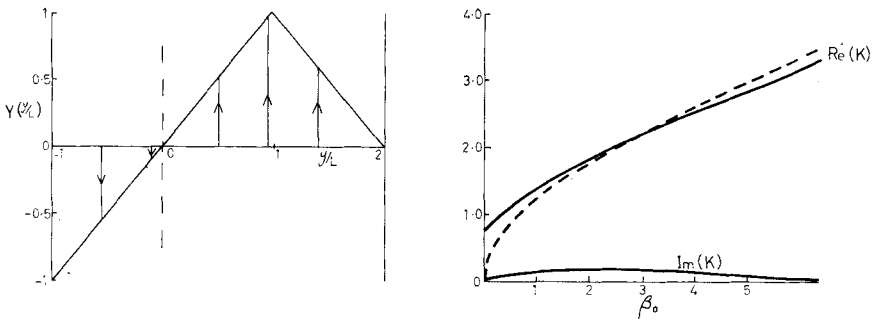

Figure 7. The latitudinal variation of a velocity profile (left) which gives singular-line absorption, and the corresponding dependence of the separation parameter κ on β_0 for a height-independent zonal flow. Solid curve: $y_l = -1$. Dashed curve: $y_l = 0$.

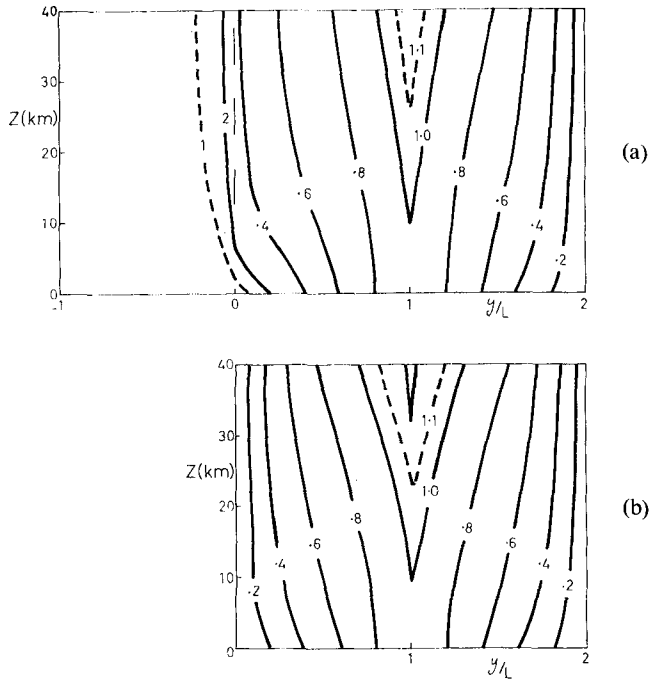

Figure 8. Meridional sections of the amplitudes of wavenumber two disturbances to the velocity profile shown on Fig. 7,

(a) With singular-line absorption; wall at $y = -L$.
(b) Without singular-line absorption; wall at $y = 0$.

In the example without singular-line absorption, wave energy is trapped, although the disturbance amplitude has a slow exponential increase with height owing to the decrease in density. The two solutions are seen to be quite similar in the region of westerly flow. Only a weak disturbance extends into the easterlies when $y_l = -1$, and the small amplitudes away from the singular line are reflected in an insensitivity of solutions to the precise negative value of y_l (Simmons 1972).

Some aspects of the meridional structure of a typical disturbance are illustrated on Fig. 9 for a velocity profile with weaker westerlies to the south of the jet maximum. Here $U_0 = 40$ m s^{-1} and $L = 25°$ latitude. Near the singular line, the solution is similar in form to that discussed by Dickinson (1968), with an energy flux $\bar{u}\,\overline{u'v'}$ towards the singular line in the region of westerly winds, and a divergence of $\overline{u'v'}$ in an infinitesimal layer at the singular line. Elsewhere, however, we note that the momentum flux is not independent of y (contrary to a conclusion of Dickinson, another consequence of his assumption of a real separation parameter), and the convergence $-\partial/\partial y\ (\overline{u'v'})$ of the Reynolds' stress is a maximum at the axis of the jet, illustrating a tendency of the forced waves to transport momentum so as to reinforce the zonal wind maximum. As found in models without a singular line, the amplitude of the disturbance is a maximum where the westerly winds are strongest. Similar conclusions result from a flow profile in which the discontinuities in latitudinal shear illustrated on Fig. 9 are removed (Simmons 1972).

Thus, in the examples presented here, absorption of wave energy due to the equatorial singular line is seen to give rise to a relatively minor reduction in the vertical penetration of planetary-scale disturbances forced in the polar winter stratosphere, and influences little

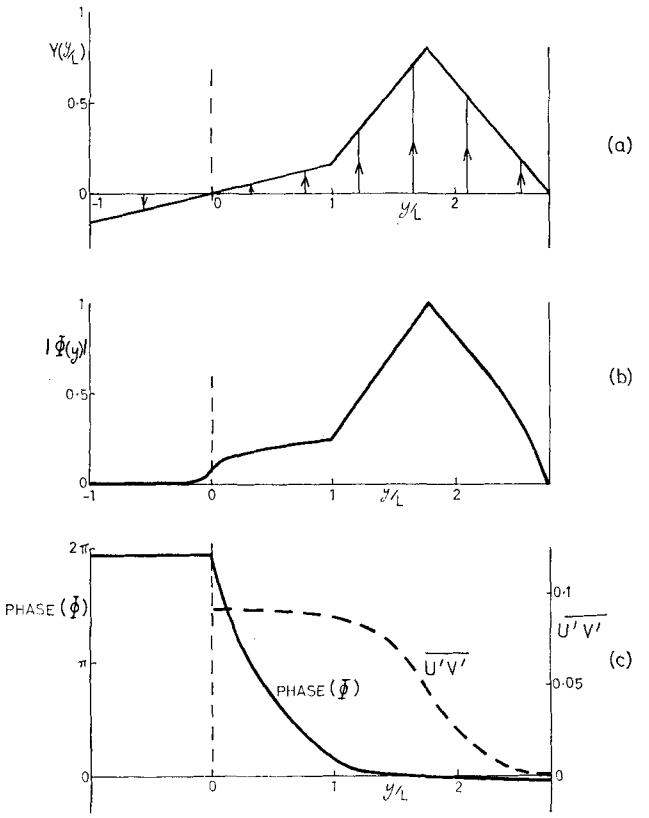

Figure 9. The latitudinal variation of a velocity profile (upper) which gives singular-line absorption, and of the amplitude (middle), and phase and momentum transport, $\overline{u'v'}$, (lower), of a typical disturbance.

the location of the latitude of maximum wave activity. Lack of a proof of completeness of the set of eigenfunctions of Eq. (12) prevents the drawing of general conclusions, but the indications seen here are confirmed by asymptotic solutions at large heights for a flow with uniform vertical shear. These are discussed in detail in Simmons (1972). For parameter values of the order used previously, such asymptotic solutions give a good estimate of the height at which wavenumber two reaches its maximum amplitude in the absence of singular-line absorption. With singular lines included as in this Section, differences of around three kilometres are found in the heights of the maxima predicted by asymptotic solutions. Amplitudes are again largest in the region of strong westerly winds.

7. Some analytical solutions for time-dependent disturbances

(a) *Formulation*

We examine the time-dependent behaviour of planetary waves forced from below in a model with uniform vertical shear, Λ, but with no meridional shear. On a β-plane of latitudinal width L, the complex amplitude of the stream function

$$Re\left\{\psi(z, t)\, e^{ikx} \sin \frac{\pi y}{L}\right\}$$

satisfies the dimensionless equation

$$\left(z - i\frac{\partial}{\partial t}\right)(\psi_{zz} - \mu\psi_z - \psi) + \mu(1 + \beta_1)\psi = 0 \quad . \quad . \quad (14)$$

where, writing $K = \sqrt{k^2 + \pi^2/L^2}$, z is scaled with f/NK, and t with $NK/f\Lambda k$. The dimensionless parameters are

$$\mu = \frac{f}{NKH_I} \qquad \text{and} \qquad \beta_1 = \frac{\beta N^2 H_I}{f^2 \Lambda} .$$

Eq. (14) is solved subject to the upper boundary condition

$$e^{-\mu z}|\psi|^2 \to 0 \quad \text{as} \quad z \to \infty ,$$

and at the lower boundary we specify the amplitude of the stream function, $\psi(z_0, t) = F(t)$ say.

An equation identical in form to (14) holds for a flow in the polar-cap geometry with a constant angular velocity in the horizontal. In this case the meridional structure of the disturbance is a Bessel rather than a sine function. The parameters μ and β_1 vary between the two geometries by less than 10 per cent for wavenumbers one and two, and similar results are found in each. In view of a quantitative deficiency in the vertical penetration of solutions which arises from the neglect of meridional mean-flow variations, it is inappropriate to dwell on the differences. Apart from Fig. 13, specific solutions illustrated subsequently relate to the polar cap, with disturbance maxima at 60°N for both wavenumber one and two.

If $\psi(z, t)$ has an $\exp(\sigma t)$ time dependence, solutions may again be found in terms of confluent hypergeometric functions. Thus, for a general forcing, the formal solution is obtained by Laplace transformation as

$$\psi(z, t) = \frac{1}{2\pi i}\int_{-i\infty}^{i\infty} e^{\sigma t}\hat{F}(\sigma)e^{-\lambda(z-z_0)}\frac{(z - i\sigma)\,U_2(\gamma, z - i\sigma)}{(z_0 - i\sigma)\,U_2(\gamma, z_0 - i\sigma)}\,d\sigma , \quad . \quad (15)$$

where $\hat{F}(\sigma)$ is the Laplace transform of the forcing function $F(t)$, and we have adopted the shorter notation

$$U_j(\gamma, z) \text{ for } U(1 - \gamma, j, 2z\sqrt{1 + \mu^2/4}) .$$

At integral values of γ, $U_2(\gamma, z)$ takes a polynomial form, and (15) may be integrated to yield relatively simple analytical expressions for the dependence of the disturbance stream function on time and height. With the parameter values used previously,

$\gamma = 1$ when $\Lambda = 3{\cdot}87$ (m s^{-1}) km^{-1} for wavenumber one,

when $\Lambda = 1{\cdot}78$ (m s^{-1}) km^{-1} for wavenumber two,

and $\gamma = 2$ when $\Lambda = 1{\cdot}03$ (m s^{-1}) km^{-1} for wavenumber one.

Integral values of γ thus occur in the parameter range of practical interest, and we discuss solutions when $\gamma = 1$ and $\gamma = 2$.

(*b*) $\gamma = 1$

When $\gamma = 1$, $U_2(\gamma, z) = 1$, and

$$\psi(z, t) = \frac{1}{2\pi i} \int_{-i\infty}^{i\infty} \hat{F}(\sigma) e^{\sigma t} \frac{z - i\sigma}{z_0 - i\sigma} e^{-\lambda(z - z_0)} \, d\sigma \, . \quad . \quad . \quad (16)$$

After some manipulation, and an application of the convolution theorem, this expression may be reduced to

$$\psi(z, t) = e^{-\lambda(z - z_0)} \{F(t) + i(z - z_0) \int_0^t F(\tau) e^{iz_0(\tau - t)} \, d\tau\} \quad . \quad . \quad (17)$$

As noted in Section 2, resonance can occur for certain forcing levels, and at $\gamma = 1$ the steady solution is unbounded when $z_0 = 0$. In this case, Eq. (17) gives

$$\psi(z, t) = e^{-\lambda z} \left\{ F(t) + iz \int_0^t F(\tau) \, d\tau \right\}, \quad . \quad . \quad . \quad (18)$$

and if $F(t) \to 1$ as $t \to \infty$, then

$$\psi(z, t) \sim itze^{-\lambda z} \text{ for large } t.$$

Thus, at resonance, the disturbance exhibits an asymptotic linear growth with time.

The solutions for wavenumber two given by Eqs. (17) and (18) are illustrated on Fig. 10, choosing $z_0 = 2$ km in the non-resonant case, and $F(t) = 1 - \exp(-\kappa t)$, with κ such that

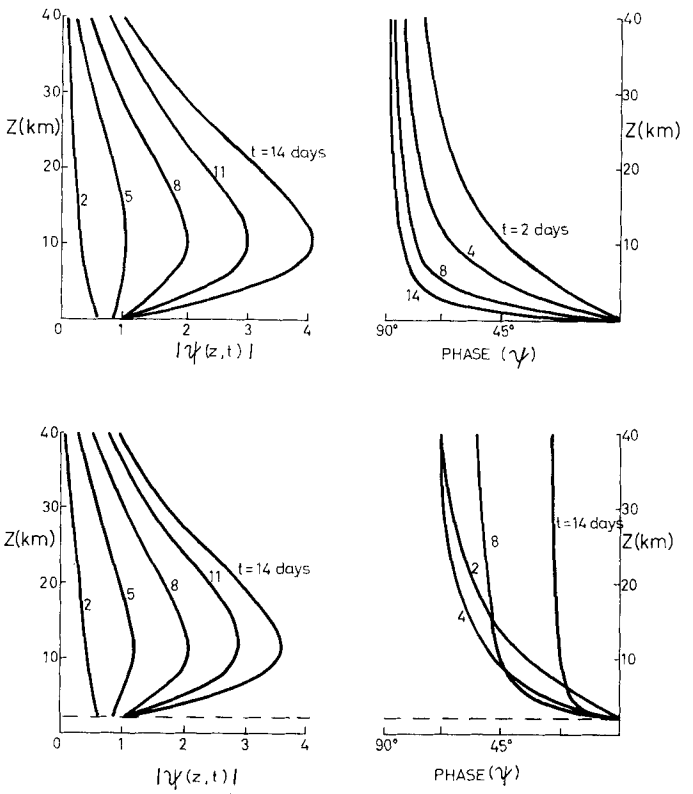

Figure 10. The variation with height and time of the amplitude (left) and phase (right) of wavenumber two solutions at $\gamma = 1$, $\Lambda = 1{\cdot}78(\text{m s}^{-1})\text{km}^{-1}$. The phase is plotted with eastward to the right.
Upper curves: Resonant growth, $z = 0$.
Lower curves: Non-resonant growth, $z_0 = 2$ km.

the forcing reaches 90 per cent of its final amplitude at day 5. The period for which the solutions are presented, 14 days, is the time scale of fluctuations in amplitude of wave-numbers one and two at the tropopause (Hirota and Sato 1969). Comparison with Fig. 2 reveals the deficient vertical penetration which results from our neglect of meridional variations of the mean flow.

On a time scale of two weeks, the amplitude of the response does not appear to depend sensitively on being at resonance. A qualitative difference between the amplitudes becomes apparent over a longer period of time, when the resonant disturbance continues to grow, while in the non-resonant case, for which the response is given largely by a free mode with eastward phase-speed, the amplitude reaches a maximum at day 19, and oscillates thereafter with a period of about 34 days.

The two solutions differ more significantly in their phases. Both show a westward tilt of troughs and ridges with increasing height, and thus, as they grow, the disturbances are drawing on the potential energy available in the mean state. Since the rate of change of disturbance amplitude is dependent on this process, subsequent differences in amplitude are preceded by differences in phase.

In the resonant example, and at small times in the non-resonant case, the level at which the disturbance has a given phase moves downward with increasing time. This is a feature of several solutions to be presented, and means that an observer at a fixed longitude would see a downward movement of a warming initially at high levels. This is the case in actual stratospheric warmings (see e.g. Teweles 1958), but we note that the apparent downward movement found in our models of small-amplitude disturbances is quite different from the actual downward movement of a strong polar warming in the non-linear regime modelled by Matsuno (1971).

(c) *The energetics of forced disturbances at* $\gamma = 1$

Our model zonal flow has vertical shear and disturbances may therefore grow gaining energy not only from any work being done at the lower boundary, but also from the potential energy of the mean state. We evaluate the proportion of eddy energy drawn from these two sources for the analytical solutions when $\gamma = 1$.

The vertical velocity, w', and perturbation pressure, p', are defined in dimensionless form by the complex amplitudes

$$\hat{w} = -i\left\{\left(z - i\frac{\partial}{\partial t}\right)\psi_z - \psi\right\},$$

and

$$\hat{p} = e^{-\mu z}\psi.$$

Apart from a common factor relating to the meridional structure of the disturbance, the net upward energy flux, $\overline{p'w'}$, is given by

$$\overline{p'w'} = \tfrac{1}{2}\,Re\,\{\hat{p}\hat{w}^*\} = \tfrac{1}{2}\,e^{-\mu z}\,Im\left\{\psi^*\left[\left(z - i\frac{\partial}{\partial t}\right)\psi_z - \psi\right]\right\},$$

and the net conversion, C, from zonal to eddy potential energy for the region above $z = z_1$ is

$$C = \tfrac{1}{2}\int_{z_1}^{\infty} e^{-\mu z}\,Im\,\{\psi_z\,\psi^*\}\,dz\,.$$

From Eq. (17), we obtain, after some manipulation,

$$\overline{p'w'} = \tfrac{1}{4}\,\lambda e^{-\mu z}\frac{\partial}{\partial t}\,\{|\psi|^2\} \qquad . \qquad . \qquad . \qquad (19)$$

and

$$C = \frac{e^{-\mu z_1} e^{-2\lambda(z_1 - z_0)}}{4(2\lambda + \mu)} \frac{\partial}{\partial t} \{|G|^2\} \quad . \quad . \quad . \quad (20)$$

where

$$G(t) = i \int_0^t F(\tau) e^{iz_0(\tau - t)} \, d\tau.$$

Eq. (19) shows that the net work done by the pressure at level z after time t has elapsed is

$$\int_0^t \overline{p'w'} \, dt = \tfrac{1}{4} \lambda e^{-\mu z} |\psi(z, t)|^2,$$

and, in particular, the net energy input at the forcing level is

$$\tfrac{1}{4} \lambda e^{-\mu z_0} |F(t)|^2.$$

Thus, at resonance, when $z_0 = 0$ and $F(t) \to 1$ as $t \to \infty$, there is only a finite amount of work, $\lambda/4$, done at the lower boundary, and the principal energy source for the unbounded response is the potential energy of the mean state. As time increases, an ever smaller fraction of the disturbance energy is supplied at the lower boundary. In the example of resonance shown on Fig. 10, the work done at the lower boundary has provided only three per cent of the eddy energy at day 14. A figure of four per cent is found after 14 days in the example with $z_0 = 2$ km.

Somewhat different conclusions might be drawn if we consider only the energetics of a region above some level z_1. For large t, at resonance,

$$\frac{\overline{p'w'}|_{z=z_1}}{C} = \lambda(2\lambda + \mu) z_1^2,$$

and this ratio increases as z_1 increases. If we take the region above 5 km, after 14 days 48 per cent of the perturbation energy in the resonant wavenumber two disturbance has been supplied from below. Above 10 km, the figure is 80 per cent. The forcing thus acts to excite a conversion of zonal available potential energy to the eddy form, this conversion taking place mostly in the lowest levels of the model. The disturbance energy is redistributed in the vertical by a correlation between pressure and vertical velocity, and a deep stratospheric wave results. The conclusions to be drawn as to the energetics of the model disturbances are seen to depend critically on the region chosen for study; similar comments apply to the energetics of observed disturbances, as emphasized by Newell and Richards (1969).

Values deduced by Newell *et al.* (1969, Fig. 13) from observations show a conversion from zonal to eddy potential energy at the base of the polar-night jet, as indicated by our calculations. The maximum magnitude of this conversion is about half that of the corresponding conversion in the mid-latitude tropospheric westerlies, but, in analyses of the energetics of the lower and middle stratosphere, it tends to be cancelled by a conversion of opposite sign above the tropospheric jet.

(*d*) $\gamma = 2$

When $\gamma = 2$,

$$U_2(\gamma, z) \propto 1 - z\sqrt{1 + \mu^2/4},$$

and, if the forcing is applied at $z = 0$, we find

$$\psi(z,t) = e^{-\lambda z}\left\{F(t) + iz\int_0^t F(\tau)d\tau - z\sqrt{1+\mu^2/4}\,H(t) - iz^2\sqrt{1+\mu^2/4}\int_0^t H(\tau)d\tau\right\},$$

where

$$H(t) = -\frac{i}{\sqrt{1+\mu^2/4}}\int_0^t F(\tau)\exp\left\{\frac{i(t-\tau)}{\sqrt{1+\mu^2/4}}\right\}d\tau\,.$$

With $F(t) = 1 - \exp(-\kappa t)$, κ as before, this solution, together with that at $\gamma = 1$, is presented for wavenumber one on Fig. 11.

The values $\gamma = 1$ and $\gamma = 2$ correspond to two quite different values of the vertical shear, but we note from Fig. 11 that there is little difference in the maximum amplitude of the response after a given time. This similarity in amplitude is discussed further in the following section. At $\gamma = 2$, the rate of working at the lower boundary, $\overline{p'w'}$, does not take the particularly simple form of Eq. (19) for $\gamma = 1$, and the conversion of zonal available potential energy accounts for only 66 per cent of the disturbance energy at day 14 in the case illustrated, in comparison with the figure of 99 per cent when $\gamma = 1$. The net amount of energy in the forced wave is less at $\gamma = 2$, the weaker shear, being about a quarter of the value at $\gamma = 1$, since the comparable maximum amplitude is attained at a higher, and therefore less dense, level.

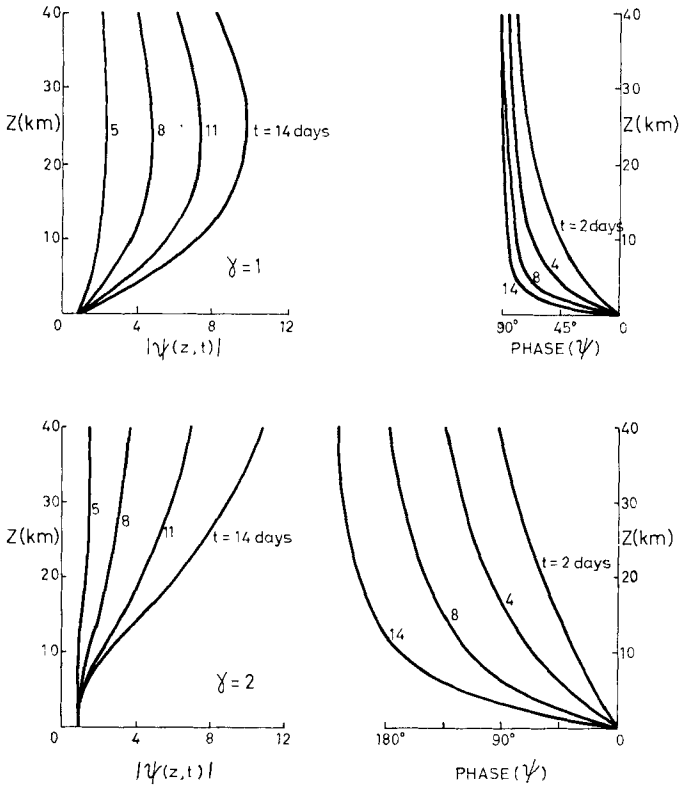

Figure 11. The variation with height and time of the amplitude (left) and phase (right) of wavenumber one solutions at $\gamma = 1$, $\Lambda = 3{\cdot}87(\mathrm{m\ s^{-1}})\mathrm{km^{-1}}$ (upper), and at $\gamma = 2$, $\Lambda = 1{\cdot}03(\mathrm{m\ s^{-1}})\mathrm{km^{-1}}$ (lower).

8. Some more general time-dependent solutions

(a) *Solutions for non-integral* γ

At non-integral γ, the formal solution (15) can be split into contributions of two types: those which arise as residues of poles of the integrand in the half-plane $Re(\sigma) \leqslant 0$, and a term arising from the logarithmic branch point of $U_2(\gamma, z)$ at the origin. To obtain the latter, we take the cut along the line $Im(z) = 0$, $Re(z) < 0$, and evaluate the loop integral around it numerically.

We illustrate the nature of the solution for the forcing $F(t) = 1 - \exp(-\kappa t)$. Then

$$\hat{F}(\sigma) = \frac{1}{\sigma} - \frac{1}{\sigma + \kappa},$$

and the integrand in (15) has singularities at

$$\sigma = 0,\ \sigma = -\kappa, \text{ and } \sigma = i(z_r - z_0),$$

where $$U_2(\gamma, z_r) = 0, \text{ and } r = 1, 2, \ldots n \text{ for } n < \gamma < n + 1.$$

When the system is not at resonance, these singularities give rise to the following contribution to the full solution:

$$\psi_a(z,t) = e^{-\lambda(z-z_0)}\left\{\frac{zU_2(\gamma,z)}{z_0U_2(\gamma,z_0)} - e^{-\kappa t}\frac{(z+i\kappa)U_2(\gamma,z+i\kappa)}{(z_0+i\kappa)U_2(\gamma,z_0+i\kappa)}\right.$$
$$\left. + \sum_{r=1}^{n}\left\{\frac{1}{z_r - z_0} - \frac{1}{z_r - z_0 - i\kappa}\right\} e^{i(z_r - z_0)t}\frac{(z + z_r - z_0)U_2(\gamma, z + z_r - z_0)}{\gamma U_1(\gamma, z_r)}\right\}. \quad (21)$$

where we have used Eq. 13.4.4 of Abramowitz and Stegun (1964) to obtain

$$\frac{d}{dz}\{zU_2(\gamma,z)\} = \gamma U_1(\gamma,z).$$

Eq. (21) describes what, for much of the parameter regime of interest, is the dominant part of the model's response. The first two terms arise from the poles of $\hat{F}(\sigma)$ at $\sigma = 0$ and $\sigma = -\kappa$, and represent directly forced modes. The additional n terms are free modes whose amplitude vanishes at the forcing level.

Further details of the solution for non-integral γ are given in Simmons (1972). The remaining term in the full expression for $\psi(z,t)$ is shown to be of the form

$$\psi_b(z,t) = \int_{-\infty}^{-z_0} H(z,s)e^{ist}\,ds,$$

with $\psi_b(z_0, t) = 0$. It describes a transient free mode with an $0(1/t)$ behaviour for large t. When $U_2(\gamma, z_0) = 0$, i.e. at resonance, the first term on the right-hand side of Eq. (21) becomes

$$\frac{e^{-\lambda(z-z_0)}}{U_1(\gamma,z_0)}\left\{U_1(\gamma,z) + \frac{z}{\gamma}\left[i\left(t - \frac{1}{\kappa}\right) - \sqrt{1 + \mu^2/4}\right]U_2(\gamma,z)\right\}.$$

There is again an asymptotic linear growth of the disturbance at resonance.

(b) *An example*

On Fig. 12, we illustrate the amplitude and phase of wavenumber one for a shear of $2(\text{m s}^{-1})\text{km}^{-1}$, which gives $\gamma = 1{\cdot}34$, with resonant forcing, $z_0 = 2{\cdot}17$ km, and non-resonant forcing, $z_0 = 0$.

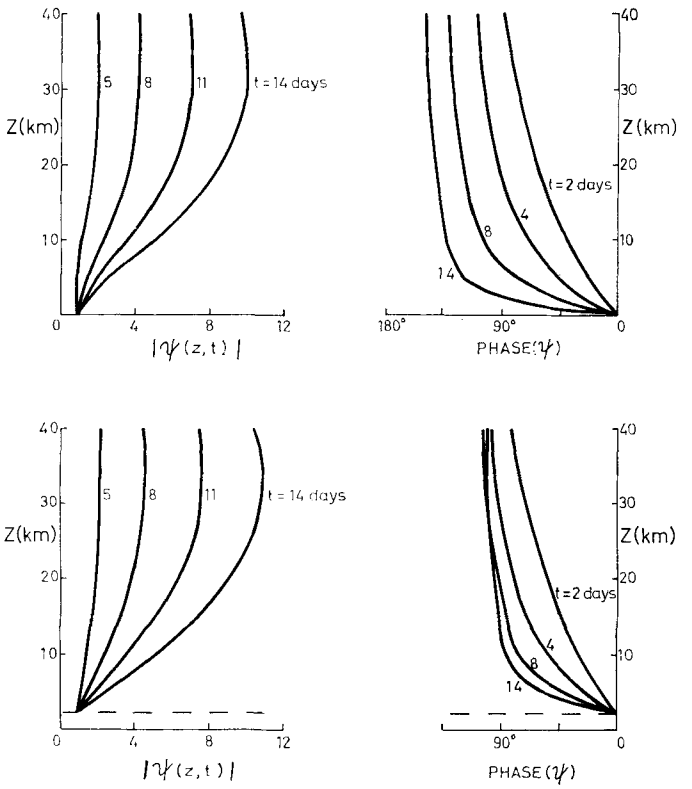

Figure 12. The variation with height and time of the amplitude (left) and phase (right) of wavenumber one solutions with

$$\Lambda = 2(\text{m s}^{-1})\text{km}^{-1} \ (\gamma = 1{\cdot}34).$$

Upper curves: non-resonant growth, $z_0 = 0$.
Lower curves: resonant growth, $z_0 = 2{\cdot}17$km.

The maximum amplitudes attained after 14 days are very similar to those shown on Fig. 11 for a much higher value of the shear ($\gamma = 1$, $\Lambda = 3{\cdot}87(\text{m s}^{-1})\text{km}^{-1}$) and a much lower one ($\gamma = 2$, $\Lambda = 1{\cdot}03(\text{m s}^{-1})\text{km}^{-1}$). Since the growing disturbances gain energy from the mean flow, when their amplitudes become large some decrease in strength of the mean flow might be expected. As linear theory suggests that amplitudes attained after a given time are relatively insensitive to the value of the vertical shear of the mean flow, there is some indication that such amplitudes may be similar to those which would be obtained from a non-linear solution, although, for the latter, we should also have to consider the generation of wavenumbers other than that directly forced at the lower boundary.

The phases of the growing waves show the westward slope, and apparent downward propagation of the disturbances, which typify our solutions. At a given level, the disturbances in general move westward as they grow, despite the stationary forcing. After an initial westward movement, an eastward movement occurs for a disturbance forced above the level which gives resonance, as in the non-resonant example shown on Fig. 10.

The bulk of the energy of the growing disturbances is drawn, at low levels, from the available potential energy of the mean state. This conversion accounts for 85 per cent of the eddy energy after 14 days for forcing at $z = 0$, 83 per cent for resonant forcing ($z_0 = 2{\cdot}17$ km), and 82 per cent when $z_0 = 4$ km. The figure of 85 per cent when $z_0 = 0$ compares with

99 per cent at the higher value of the shear ($\gamma = 1$) and 66 per cent when $\gamma = 2$. The work done by the forcing is particularly small when $\gamma = 1$, but when $\gamma = 1{\cdot}34$ it is of a similar magnitude to that when $\gamma = 2$, with less energy converted from the mean state at the weaker shear, for which less energy is available.

(c) *The inclusion of Newtonian cooling*

The formal solution in the presence of a height-independent Newtonian cooling is

$$\psi(z,t) = \frac{1}{2\pi i}\int_{-i\infty}^{i\infty} e^{\sigma t}\hat{F}(\sigma)e^{-\lambda(z-z_0)}\frac{[z-i(\sigma+\chi)]\,U_2(\gamma_c, z-i(\sigma+\chi))}{[z_0-i(\sigma+\chi)]\,U_2(\gamma_c, z_0-i(\sigma+\chi))}\,d\sigma \quad . \quad (22)$$

where $\gamma_c = \gamma - i\chi/2\sqrt{1+\mu^2/4}$, and the cooling parameter χ is scaled by $f\Lambda k/NK$. This integral may be evaluated in the same manner as described in subsection (*a*). The branch-cut transient, $\psi_b(z,t)$, is now obtained by integrating along the line $\sigma = -\chi + is$, $-z_0 > s > -\infty$, and decays more rapidly, with an $O(1/t)e^{-\chi t}$ behaviour for large t. The other free modes are now damped, but not by a simple $\exp(-\chi t)$ factor since the roots of $U_2(\gamma_c, z) = 0$ are found generally to be complex.

A number of solutions with Newtonian cooling have been presented in Simmons (1972). Amplitudes attained after a given time are found to be significantly attenuated by the inclusion of Newtonian cooling, with reductions over a 14 day period typically by a factor of $\frac{3}{4}$ for a cooling time of 14 days, and $\frac{1}{2}$ for a 7 day cooling time. This contrasts with the relatively small reduction in amplitude of the steady solutions away from resonance presented in Section 5. The difference is due mostly to the damping of free modes. In examples such as those shown on Fig. 12, these modes are initially out of phase with the steady component of the solution, and their damping by Newtonian cooling prevents the reinforcement of the steady component which occurs subsequently in adiabatic solutions.

(d) *Transient disturbances in flows with meridional variations*

Owing to our neglect of meridional variations of the mean flow, the time-dependent solutions presented hitherto do not bear close comparison with observation. We may, however, easily extend these results in an approximation in which we solve for a latitudinally-uniform zonal flow, but with the total wavenumber, $\sqrt{k^2+\pi^2/L^2}$, replaced by the zonal wavenumber, k, β by $4\beta/\pi$, and the cooling parameter χ by $4\chi/\pi$. The factor $4/\pi$ is that appropriate to a sinusoidal meridional variation of the stratospheric jet, and it has been seen in Sections 3 and 4 that this gives a good approximation to the steady component of the full solution for realistic parameter values. Some error is introduced into the phase speeds of the free modes, but comparison with a more accurate solution suggests that this results in no significant error over a time scale of two weeks (Simmons 1972).

Time-height cross-sections of wave amplitude at northern latitudes presented by Muench (1965) and Hirota and Sato (1969) reveal fluctuations which typically occur with a period of about two weeks. It is of interest to model one such transient disturbance, and we take

$$F(t) = 16e^{-2\kappa t}\{1 - 2e^{-\kappa t} + e^{-2\kappa t}\},$$

with κ chosen such that a maximum is reached at day 7. On Fig. 13 we present time-height sections of the resulting amplitude of wavenumber two, $\Lambda = 2(\mathrm{m\,s^{-1}})\mathrm{km}^{-1}$, and wavenumber one, $\Lambda = 2{\cdot}25(\mathrm{m\,s^{-1}})\mathrm{km}^{-1}$, for a β-plane centred at 60°N and a cooling time of 7 days. The slightly larger shear was used for wavenumber one since the branch-cut transient was

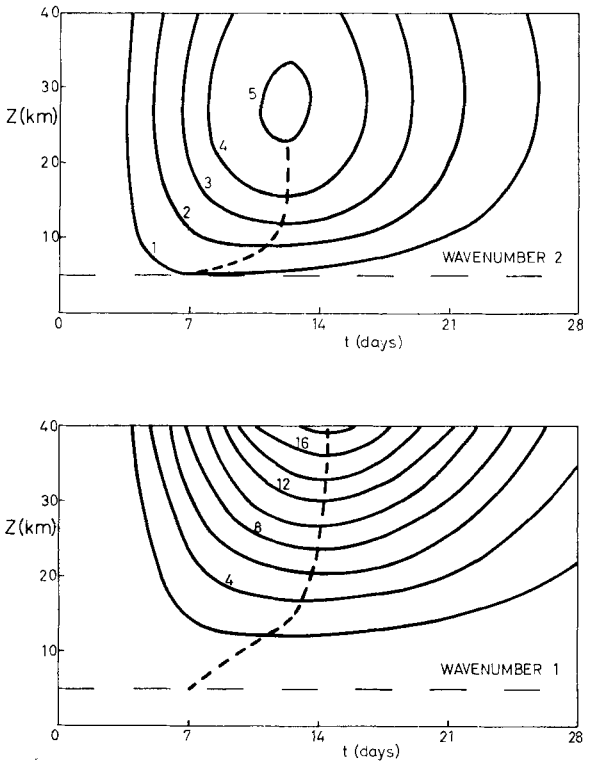

Figure 13. Time-height cross-sections of wave amplitude for a transient forcing with allowance for meridional curvature of the mean flow profile as specified in the text.

Upper: wavenumber two, $A = 2(\text{m s}^{-1})\text{km}^{-1}$.
Lower: wavenumber one, $A = 2{\cdot}25(\text{m s}^{-1})\text{km}^{-1}$.

found to be an important term when $\Lambda = 2(\text{m s}^{-1})\text{km}^{-1}$, and its numerical evaluation did not attain a sufficient accuracy.

In response to changes at the forcing level, a disturbance builds up in the stratosphere, reaching, for wavenumber two, a maximum some five days after the forcing. Subsequently, in this damped system, the wave decays to zero following the forcing. A time-lag of a week is found for wavenumber one. At $z = 20$ km, which we regard as equivalent to the 10 mb level, there is a four-fold increase in the amplitude of wavenumber two relative to its value at the forcing level, and there is a six-fold increase for wavenumber one.

These results are in reasonable agreement with the observed sections of Muench, and Hirota and Sato, both in respect of the time-lag and the amplitude attained. We note, however, that this agreement is achieved with a cooling time of 7 days. Use of a longer cooling time results in a longer delay in the stratospheric response, and larger amplitudes.

9. Conclusions

Some idealized analytical models of steady planetary-scale motions in the polar winter stratosphere have been seen to give a description of the structure of low-wavenumber disturbances which is in good agreement with observations in the lower and middle stratosphere. Contrary to a suggestion of Matsuno (1970), it has not been found necessary to invoke non-linear effects to obtain an agreement between theory and observation regarding the vertical penetration of wavenumber two. Above 30 km, our results, particularly

with respect to wavenumber two, remain to be tested against detailed observations.

Comparison of those solutions which include meridional shear with results of Charney and Drazin (1961) for a latitudinally-uniform zonal flow reveals little qualitative difference. There is, however, a marked quantitative change, illustrating the importance of the meridional curvature of the flow profile in determining the vertical penetration of disturbances forced from below. This vertical penetration is seen in a number of examples to be insensitive to the inclusion of either Newtonian cooling or an absorption of wave energy owing to an equatorial zero-wind line. Newtonian cooling does affect sensitively the heat transported polewards by a steady disturbance, and the associated conversion of zonal to eddy available potential energy accounts for much of the energy required to maintain the wave against radiative dissipation.

We have considered zonal flows limited to the form given by Eq. (3), and have thus not taken into account variations in the latitudinal extent of the winter stratospheric jet. However, our results show that, over a range of jet-like velocity profiles, the meridional variation of the pressure perturbation is similar to that of the mean zonal wind. In addition the vertical structure of the forced disturbances is insensitive both to the width of the westerly jet, and to its detailed latitudinal structure. Such results suggest that different conclusions would not be obtained from models with a more general distribution of zonal winds. Some confirmation of this is given by Eq. (10), which highlights a general similarity in structure of the zonal wind and low-wavenumber pressure disturbance in regions of strong curvature of the mean flow profile.

Both analytical and numerical solutions have been obtained for time-dependent disturbances to a flow with uniform vertical shear. With no allowance for latitudinal variations of the mean flow these solutions give a qualitative picture of the response of the stratosphere to changes in the tropospheric circulation, in which, as a disturbance grows, potential energy is converted from the mean state at low levels, and redistributed in the vertical through a positive correlation of pressure and vertical velocity. In this respect, the stratosphere appears to act as an amplifier of disturbance energy introduced at its lower boundary. Although the energy conversion is similar, the mechanism considered here is not the same as that of baroclinic instability, which depends critically on the existence of opposing potential vorticity gradients (Bretherton 1966), and which typically favours the growth of waves with shorter length scales than those predominantly observed (McIntyre 1972; Green 1972).

With some account taken of the effects of the meridional structure of the stratospheric jet, we have obtained a reasonable agreement between theory and observation for transient disturbances. The maximum value of the amplitude of wavenumber two at 10 mb is found theoretically to be about four times that reached near the model tropopause. While we cannot expect our linear model to simulate the rapid polar warming as modelled by Matsuno (1971), it is of interest to note that, using observed values for the amplitudes at the forcing level, amplitudes attained by the perturbation geopotentials are not only close to those observed for minor disturbances in the polar stratosphere, but are also close to those found for the sudden warmings of both 1958 (see Muench 1965) and 1963 (Hirota and Sato 1969). The linear model does not strictly apply in these cases, but the apparent similarity between theory and observation might be explained by our finding that the amplitude attained after a given time is insensitive to the value of the vertical shear of the mean flow, which, in reality weakens as the disturbance becomes large. Our results confirm the impression which observations give, namely that the large-amplitude pressure perturbations with which are associated sudden polar warmings are merely a response, such as described by linear theory, to an anomalously large tropospheric forcing, rather than an anomalous response occurring when the stratosphere attains a certain critical state.

ACKNOWLEDGMENTS

This work was mostly carried out at the Department of Applied Mathematics and Theoretical Physics, University of Cambridge, and completed at the Department of Geophysics, University of Reading. The continued interest and advice of Dr. M. E. McIntyre is gratefully acknowledged, as is the receipt of a research studentship from the Natural Environment Research Council. Thanks are also due to Dr. I. Hirota for permission to reproduce Fig. 1.

REFERENCES

Abramowitz, M. and Stegun, I. A. 1964 'A handbook of mathematical functions,' U.S. National Bureau of Standards.

Anderson, C. E. 1964 'Heat transport by large-scale atmospheric waves during October 1959–March 1960,' McGill Univ. Pub. in Met. No. 69.

Barnett, J. J., Cross, M. J., Harwood, R. S., Houghton, J. T., Morgan, C. G., Peckham, G. E., Rodgers, C. D., Smith, S. D. and Williamson, E. J. 1972 'The first year of the selective chopper radiometer on Nimbus 4,' *Quart. J. R. Met. Soc.*, **98**, pp. 17–37.

Blake, D. and Lindzen, R. S. 1973 'The effect of photochemical models on calculated equilibria and cooling rates in the stratosphere.' To appear.

Bretherton, F. P. 1966 'Baroclinic instability and the short wavelength cut-off in terms of potential vorticity,' *Quart. J. R. Met. Soc.*, **92**, pp. 335–345.

Byron-Scott, R. 1967 'A stratospheric general circulation experiment incorporating diabatic heating and ozone photochemistry,' McGill Univ., Pub. in Met. No. 87.

Charney, J. G. and Drazin, P. G. 1961 'Propagation of planetary-scale disturbances from the lower into the upper atmosphere,' *J. Geophys. Res.*, **66**, pp. 83–109.

Clark, J. H. E. 1972 'The vertical propagation of forced atmospheric planetary waves,' *J. Atmos. Sci.*, **29**, pp. 1,430–1,451.

Dickinson, R. E. 1968 'Planetary Rossby waves propagating vertically through weak westerly wind wave guides,' *Ibid.*, **25**, pp. 984–1,002.

1969 'Vertical propagation of planetary Rossby waves through an atmosphere with Newtonian cooling,' *J. Geophys. Res.*, **74**, pp. 929–938.

1970 'Development of a Rossby wave critical level,' *J. Atmos. Sci.*, **27**, pp. 627–633.

Green, J. S. A. 1972 'Large-scale motion in the upper stratosphere and mesosphere: an evaluation of data and theories,' *Phil. Trans. R. Soc. Lond.*, A **271**, pp. 577–583.

Hirota, I. 1971 'Excitation of planetary Rossby waves in the winter stratosphere by periodic forcing,' *J. Met. Soc. Japan*, **49**, pp. 439–449.

Hirota, I. and Sato, Y. 1969 'Periodic variation of the winter stratospheric circulation and intermittent vertical propagation of planetary waves,' *Ibid.*, **46**, pp. 418–430.

Labitzke, K. 1972 'The interaction between stratosphere and mesosphere in winter,' *J. Atmos. Sci.*, **29**, pp. 1,395–1,399.

Lindzen, R. S. and Goody, R. M. 1965 'Radiative and photochemical processes in mesospheric dynamics. Part I: Models for radiative and photochemical processes,' *Ibid.*, **22**, pp. 341–348.

Manabe, S. and Hunt, B. G. 1968 'Experiments with a stratospheric general circulation model: I. Radiative and dynamical aspects,' *Mon. Weath. Rev.*, **96**, pp. 477–502.

Matsuno, T. 1970 'Vertical propagation of stationary planetary waves in the winter northern hemisphere,' *J. Atmos. Sci.*, **27**, pp. 871–883.

1971 'A dynamical model of the stratospheric sudden warming,' *Ibid.*, **28**, pp. 1,479–1,494.

McIntyre, M. E. 1972 'Baroclinic instability of an idealized model of the polar night jet,' *Quart. J. R. Met. Soc.*, **98**, pp. 165–174.

Miyakoda, K., Strickler, R. F. and Hembree, G. D. 1970 'Numerical simulation of the breakdown of the polar-night vortex in the stratosphere,' *J. Atmos. Sci.*, **27**, pp. 139–154.

Muench, H. S. 1965 'On the dynamics of the wintertime stratospheric circulation,' *Ibid.*, **22**, pp. 340–360.

Murgatroyd, R. J. 1969 'The structure and dynamics of the stratosphere,' in *The global circulation of the atmosphere*, pub. by R. Met. Soc.

Newell, R. E. and Richards, M. E. 1969 'Energy flux and convergence patterns in the lower and middle stratosphere during the IQSY,' *Quart. J. R. Met. Soc.*, **95**, pp. 310–328.

Newell, R. E., Vincent, D. G., Dopplick, T. G., Ferruzza, D. and Kidson, J. W. 1969 'The energy balance of the global atmosphere,' in *The global circulation of the atmosphere*, pub. by R. Met. Soc.

Sawyer, J. S. 1965 'The dynamical problems of the lower stratosphere,' *Quart. J. R. Met. Soc.*, **91**, pp. 407–416.

Scherhag, R. 1952 'Die explosionsartigen Stratosphärenerwarmungen des Spätwinters 1951–1952,' *Ber. Deut. Wetterd.*, **6**, pp. 51–63.

Simmons, A. J. 1972 'Baroclinic instability and planetary waves in the polar stratosphere,' Ph.D. thesis, Univ. of Cambridge.

Teweles, S. 1958 'Anomalous warming of the stratosphere over North America in early 1957,' *Mon. Weath. Rev.*, **86**, pp. 377–396.

APPENDIX

(*a*) *The sinusoidal jet*

We consider flow on a β-plane with

$$\bar{u}(y, z) = \Lambda z \sin \frac{\pi y}{L}, \quad 0 < y < L .$$

It will later be shown that the problem for a more general mean flow $\Lambda z Y(y)$, and that for a flow in the polar cap geometry with height-independent vertical shear, may be transformed into that considered here.

We form a Fourier expansion of the stream function:

$$\psi(y, z) = \sum_1^\infty \psi_n(z) \sin \frac{n\pi y}{L}, \qquad . \quad . \quad . \quad \text{(A.1)}$$

and consider explicitly only the simplest case of a sinusoidal forcing:

$$\psi_n(z_0) = 0 \text{ for } n > 1.$$

Substituting the form (A.1) into Eq. (1), we obtain the following set of coupled ordinary differential equations for the ψ_n:

$$z\{\psi_{nzz} - \mu\psi_{nz} - [1 + (n^2 - 1)\varepsilon]\psi_n\} + \mu\psi_n + \mu\beta_* \sum_1^\infty S_{nm}\psi_m = 0 \; . \qquad . \quad \text{(A.2)}$$

where we have scaled z with $\alpha = Nk/f$, and

$$\varepsilon = \frac{\pi^2}{k^2 L^2}, \; \mu = \frac{1}{\alpha H_I}, \text{ and } \beta_* = \frac{4\beta N^2 H_I}{\pi f^2 \Lambda} .$$

$$S_{nm} = S_{mn} = \frac{\pi}{2} \int_0^1 \frac{\sin m\pi y \sin n\pi y}{\sin \pi y} \, dy .$$

The coupling in the set (A.2) arise solely from the β-term, consistent with the separable solution (4) when $\beta = 0$.

Since only odd modes are generated, we may set

$$\psi_{2n-1} = \Psi_n e^{\mu z/2},$$

$$B_{nm} = \mu\delta_{nm} + \mu\beta_* S_{2n-1,2m-1},$$

and we obtain from (A.2) the set

$$\Psi_{nzz} = \left\{1 + \frac{\mu^2}{4} + 4(n^2 - n)\varepsilon\right\}\Psi_n - \frac{1}{z}\sum_{m=1}^{\infty} B_{nm}\Psi_m . \quad . \quad . \quad (A.3)$$

We use the relatively large magnitude of the factor $\{1 + \mu^2/4 + 4(n^2 - n)\varepsilon\}$ when $n \geqslant 2$ to obtain approximate expressions for Ψ_n, $n \geqslant 2$, in terms of Ψ_1. Substituting these expressions into (A.3) for the case $n = 1$ allows the solution for Ψ_1 to be found either analytically or numerically, depending on the degree of approximation invoked. Formally, our results are valid in the limit $\varepsilon = \pi^2/k^2L^2 \to \infty$, a "narrow-channel" approximation, but in practice the method works well for parameter values appropriate to the polar-night vortex, for, with $L = 40°$ latitude, and wavenumber 2 at 60°N, $\varepsilon = 1{\cdot}21$, and the small parameters in our expansions,

$$\mu_n = \frac{\mu\beta_*}{1 + \mu^2/4 + 4(n^2 - n)\varepsilon}, \quad n > 1,$$

have a maximum value of 0·17 when $n = 2$, for $\Lambda = 2(\mathrm{m\,s^{-1}})\mathrm{km}^{-1}$ and other parameter values as used throughout.

To lowest order,

$$\Psi_n^{(1)} = 0, \; n > 1,$$

and the 0(1) approximation to Ψ_1, $\Psi_1^{(1)}$, is precisely that given by Eq. (8).

Using Eq. (A.3), and writing

$$B_{1n} = \frac{\mu\beta_*}{(2n-1)},$$

the second approximation introduces the other horizontal modes through

$$\Psi_n^{(2)} = \mu_n \frac{\mu\beta_*}{(2n-1)}\left\{\frac{\Psi_1^{(2)}(z)}{z} - \frac{\Psi_1(z_0)}{z_0}\phi_n(z)\right\}, n > 1, \quad . \quad . \quad (A.4)$$

where, for analytical ease, we retain Ψ_1 to second order on the right-hand side, and

$$\phi_n = e^{-(\mu/2 + \lambda_n)z}\frac{zU(1 - \gamma_n, 2, \chi_n z)}{z_0 U(1 - \gamma_n, 2, \chi_n z_0)},$$

with

$$\lambda_n = -\frac{\mu}{2} + \sqrt{1 + \mu^2/4 + 4(n^2 - n)\varepsilon},$$

$$\chi_n = 2\sqrt{1 + \mu^2/4 + 4(n^2 - n)\varepsilon},$$

and

$$\gamma_n = \frac{\mu(1 + \beta_* S_{nn})}{\chi_n}.$$

The approximation (A.4) for Ψ_n illustrates the particularly weak coupling at large z, with $\phi_n(z)$ tending to zero much more rapidly than $\Psi_1^{(2)}$ as $\mu_n \to 0$. We avoid difficulties for small z by restricting the forcing level to be some distance above $z = 0$.

Substituting (A.4) into (A.3) we obtain the following equation for $\Psi_1^{(2)}$:

$$\Psi_{1zz}^{(2)} - \left(1 + \frac{\mu^2}{4} - \frac{\mu(1+\beta_*)}{z} - \frac{1}{z^2} S_1\right) \Psi_1^{(2)} = \frac{\mu\beta_*}{zz_0} \Psi_1(z_0) \sum_2^\infty \mu_n \frac{\phi_n}{(2n-1)^2}, \quad . \quad \text{(A.5)}$$

where

$$S_1 = \sum_2^\infty \mu_n \frac{\mu\beta_*}{(2n-1)^2}.$$

The inhomogeneous term on the right-hand side of (A.5) has a rapid exponential decay with increasing z, and the particular integral is $0(\mu_2^2)$ as μ_2 (and thus μ_n) $\to 0$. Thus $\Psi_1^{(2)}$ is given by the solution of (A.5) with the right-hand side set to zero, and, since this is now Whittaker's equation, we have

$$\Psi_1^{(2)} = e^{-(\lambda + \mu/2)(z-z_0)} \Psi_1(z_0) \left(\frac{z}{z_0}\right)^{1-S_1} \frac{U(1-\gamma-S_1, 2-2S_1, 2z\sqrt{1+\mu^2/4})}{U(1-\gamma-S_1, 2-2S_1, 2z_0\sqrt{1+\mu^2/4})}, \quad \text{(A.6)}$$

where terms $0(S_1^2)$ have been consistently neglected. Eq. (A.6), together with expression (A.4) for $\Psi_n^{(2)}$ in terms of $\Psi_1^{(2)}$, thus yields a further analytical approximation to the required solution. As $S_1 \to 0$, we recover from (A.6) the lowest-order solution (8).

A number of further approximations have been developed. The expansion presented in this appendix has been taken to a further order in μ_2, in which case the resulting ordinary differential equation for $\Psi_1^{(3)}$ has been solved numerically. Solutions obtained in this manner have been compared with those obtained by finding analytical expressions for $\Psi_n (n \geqslant 3)$ in terms of Ψ_1 and Ψ_2, and solving numerically the pair of coupled ordinary differential equations for Ψ_1 and Ψ_2, and with those obtained in terms of power series expansions in z. Some details are given in Simmons (1972). In general, the resulting values of the disturbance amplitude close to its maximum have been found to agree to within 1 per cent.

(*b*) *A more general horizontal profile*

When

$$\bar{u}(y,z) = \Lambda z Y(y/L),$$

the spectral coefficients $\psi_n(z)$ in expansion (A.1) satisfy the coupled set

$$z\{\psi_{nzz} - \mu\psi_{nz} - (1 + n^2\varepsilon)\psi_n\} + \sum_{m=1}^{\infty} (B_{nm} + \varepsilon z A_{nm})\psi_m = 0 \quad . \quad \text{(A.7)}$$

where

$$B_{nm} = \mu\delta_{nm} + \mu\beta_* \frac{\pi}{2} \int_0^1 \frac{\sin n\pi t \sin m\pi t}{Y(t)}\, dt,$$

and

$$A_{nm} = -\frac{2}{\pi^2} \int_0^1 \frac{Y''}{Y} \sin n\pi t \sin m\pi t\, dt$$

We transform the set (A.7) into the form (A.2) derived for the sinusoidal jet, in which case the methods of solution outlined in subsection (*a*) apply.

We introduce the eigenvalues of the matrix

$$(1 + n^2\varepsilon)\delta_{nm} - A_{nm} ,$$

as

$$t_s, (s = 1,2, \ldots), \text{ with corresponding eigenvectors } \lambda_{si}.$$

Defining

$$\Psi_p = \sum_{m=1}^{\infty} \lambda_{pm}\psi_m ,$$

we obtain from (A.7) the set

$$z(\Psi_{szz} - \mu\Psi_{sz} - t_s\Psi_s) + \sum_{q=1}^{\infty} M_{sq}\Psi_q = 0 \quad . \quad . \quad . \quad \text{(A.8)}$$

where

$$M_{sq} = \sum_{m=1}^{\infty}\sum_{n=1}^{\infty} \lambda_{sn}B_{nm}L_{mq}$$

and L_{mq} is such that $\sum_{m=1}^{\infty} \lambda_{sm}L_{mq} = \delta_{sq}$.

The set (A.8) is precisely of the form of (A.2), and, having solved for Ψ_n, ψ_n is obtained by the transformation

$$\psi_n = \sum_{q=1}^{\infty} L_{nq}\Psi_q$$

(*c*) *The polar-cap geometry*

Similar expansions may be carried out in other geometries. We illustrate for the polar cap introduced in Section 3(*c*).

For a zonal flow

$$\bar{u}(r,z) = \Lambda zrw(r)$$

the time-independent stream function $\psi(r,z)e^{in\Phi}$ satisfies

$$\Lambda zw\left\{\frac{1}{\rho}\left(\frac{\rho f^2}{N^2}\psi_z\right)_z + \frac{1}{r}(r\psi_r)_r - \frac{n^2}{r^2}\psi\right\}$$

$$+ \left\{\beta - \Lambda z\left(w_{rr} + \frac{3}{r}w_r\right) + w\frac{\Lambda f^2}{N^2H_I}\right\}\psi = 0 \qquad \text{(A.9)}$$

where $\beta = f/a^2$.

We expand

$$\psi = \sum_{m=1}^{\infty} \psi_m(z)J_n(\lambda_{nm}r/R_0)$$

where R_0 is the radius of the boundary wall imposed on the model, and λ_{nm} is the mth zero of J_n. We form the Fourier-Bessel expansions

$$\frac{1}{w} J_n\left(\lambda_{nm} \frac{r}{R_0}\right) = R_0 \sum_{s=1}^{\infty} B_{nsm} J_n\left(\lambda_{ns} \frac{r}{R_0}\right),$$

and

$$\frac{1}{w}\left(w_{rr} + \frac{3}{r} w_r\right) J_n\left(\lambda_{nm} \frac{r}{R_0}\right) = \frac{1}{R_0^2} \sum_{s=1}^{\infty} A_{nsm} J_n\left(\lambda_{ns} \frac{r}{R_0}\right).$$

Eq. (A.9) is then reduced to the following set of coupled ordinary differential equations:

$$\Lambda z\left\{\frac{1}{\rho}\left(\frac{\rho f^2}{N^2} \psi_{mz}\right)_z - \frac{1}{R_0^2} \lambda_{nm}^2 \psi_m\right\} + \beta R_0 \sum_{s=1}^{\infty} B_{nms} \psi_s - \frac{\Lambda}{R_0^2} z \sum_{s=1}^{\infty} A_{nms} \psi_s + \frac{f^2 \Lambda}{N^2 H_I} \psi_m = 0.$$

For fixed zonal wavenumber n, when appropriately scaled, the above set is precisely of the form (A.8), and may be solved as described in subsections (*a*) and (*b*).